REPORT DOCUMENTATION PAGE

Form Approved OMB NO. 0704-0188

1. REPORT DATE (DD-MM-YYYY)	2. REPORT TYPE	3. DATES COVERED (From - To)
10-04-2014	Final Report	1-Oct-2010 - 31-Dec-2013

4. TITLE AND SUBTITLE
Novel Structural Health Monitoring Schemes for Glass-Fiber Composites using Nanofillers

5a. CONTRACT NUMBER	W911NF-10-1-0267
5b. GRANT NUMBER	
5c. PROGRAM ELEMENT NUMBER	611102
5d. PROJECT NUMBER	
5e. TASK NUMBER	
5f. WORK UNIT NUMBER	

6. AUTHORS
Charles E. Bakis, Kon-Well Wang

7. PERFORMING ORGANIZATION NAMES AND ADDRESSES
Pennsylvania State University
Office of Sponsored Programs
110 Technology Center
University Park, PA 16802 -7000

8. PERFORMING ORGANIZATION REPORT NUMBER

9. SPONSORING/MONITORING AGENCY NAME(S) AND ADDRESS (ES)
U.S. Army Research Office
P.O. Box 12211
Research Triangle Park, NC 27709-2211

10. SPONSOR/MONITOR'S ACRONYM(S)
ARO

11. SPONSOR/MONITOR'S REPORT NUMBER(S)
58085-EG.10

12. DISTRIBUTION AVAILIBILITY STATEMENT
Approved for Public Release; Distribution Unlimited

13. SUPPLEMENTARY NOTES
The views, opinions and/or findings contained in this report are those of the author(s) and should not contrued as an official Department of the Army position, policy or decision, unless so designated by other documentation.

14. ABSTRACT
The objective of the investigation is to explore a new approach for high sensitivity structural health monitoring of continuous glass fiber reinforced polymer composites (GFRPs). Conductive nanofillers were used for tailoring the anisotropic conductivity of GFRP. Carbon nanotubes and carbon blacks were anisotropically networked using dielectrophoretic manipulation during processing. Smaller, low-aspect-ratio nanofillers (carbon black) in low concentrations were superior to high-aspect-ratio nanofillers (nanotubes) for electrical tailoring purposes. Networking of carbon black nanoparticles through the thickness increased the detectability of delamination

15. SUBJECT TERMS
Structural Health Monitoring, Damage Detection, Composite Materials, Nanocomposites, Electrical Properties

16. SECURITY CLASSIFICATION OF:			17. LIMITATION OF ABSTRACT	15. NUMBER OF PAGES	19a. NAME OF RESPONSIBLE PERSON
a. REPORT	b. ABSTRACT	c. THIS PAGE			Charles Bakis
UU	UU	UU	UU		19b. TELEPHONE NUMBER: 814-865-3178

Report Title

Novel Structural Health Monitoring Schemes for Glass-Fiber Composites using Nanofillers

ABSTRACT

The objective of the investigation is to explore a new approach for high sensitivity structural health monitoring of continuous glass fiber reinforced polymer composites (GFRPs). Conductive nanofillers were used for tailoring the anisotropic conductivity of GFRP. Carbon nanotubes and carbon blacks were anisotropically networked using dielectrophoretic manipulation during processing. Smaller, low-aspect-ratio nanofillers (carbon black) in low concentrations were superior to high-aspect-ratio nanofillers (nanotubes) for electrical tailoring purposes. Networking of carbon black nanoparticles through the thickness increased the detectability of delamination. Electrical impedance tomography (EIT) was shown to be able to accurately locate through-hole damage as small as 3.18 mm in diameter as well as impact damage to a GFRP laminate with aligned carbon black. EIT has also been used to locate damage in a carbon nanofiber (CNF) filled epoxy composite. Methods of improving EIT for structural health monitoring of nanocomposites have been investigated. Experimentally, utilizing the conductivity evolution of CNF/epoxy for baseline free damage detection has been explored. Analytically, it has been shown that piezoresistive coupling and nanofiller alignment both enhance the ability of EIT to detect damage.

Enter List of papers submitted or published that acknowledge ARO support from the start of the project to the date of this printing. List the papers, including journal references, in the following categories:

(a) Papers published in peer-reviewed journals (N/A for none)

Received		Paper
03/21/2012	1.00	Ye Zhu, Charles E. Bakis, James H. Adair. Effects of carbon nanofiller functionalization and distribution on interlaminar fracture toughness of multi-scale reinforced polymer composites, Carbon, (03 2012): 0. doi: 10.1016/j.carbon.2011.11.001
04/10/2014	8.00	S. Gungor, C. E. Bakis. Anisotropic networking of carbon black in glass/epoxy composites using electric field, Journal of Composite Materials, (02 2014): 0. doi: 10.1177/0021998314521256
04/10/2014	7.00	T N Tallman, S Gungor, K W Wang, C E Bakis. Damage detection and conductivity evolution in carbon nanofiber epoxy via electrical impedance tomography, Smart Materials and Structures, (04 2014): 0. doi: 10.1088/0964-1726/23/4/045034
09/01/2013	4.00	T. Tallman, K. W. Wang. An arbitrary strains carbon nanotube composite piezoresistivity model for finite element integration, Applied Physics Letters, (01 2013): 0. doi: 10.1063/1.4774294
TOTAL:	**4**	

Number of Papers published in peer-reviewed journals:

(b) Papers published in non-peer-reviewed journals (N/A for none)

Received	Paper

TOTAL:

Number of Papers published in non peer-reviewed journals:

(c) Presentations

Number of Presentations: 0.00

Non Peer-Reviewed Conference Proceeding publications (other than abstracts):

Received		Paper
04/10/2014	9.00	T. Tallman, F. Semperlotti, K.W. Wang. Enhanced Damage Detection in Conductive Polymer-based Composites through Piezoresistive Coupling, 28th Technical Conference, American Society for Composites. 09-SEP-13, . : ,
08/31/2012	3.00	Tyler Tallman, Fabio Semperlotti, Kon Well Wang. Enhanced Health Monitoring of Fibrous Composites with Aligned Carbon Nano-Tube Networks and Electrical Impedance Tomography, SPIE – Society of Photo-Optical Instrumentation Engineers, Health Monitoring of Structural and Biological Systems Conference. , . : ,

TOTAL: **2**

Number of Non Peer-Reviewed Conference Proceeding publications (other than abstracts):

Peer-Reviewed Conference Proceeding publications (other than abstracts):

Received		Paper
08/31/2012	2.00	Ye Zhu, Charles E. Bakis. CAI Strength of Filament Wound Glass Fiber Composites Toughened with Carbon Nanofillers, SAMPE 2012 Conference and Exposition. 22-MAY-12, . : ,
09/01/2013	5.00	Sila Gungor, Charles E. Bakis . Electrical Anisotropy of Unidirectional Glass Fiber Reinforced Composites Containing Carbon Black, Proc. SAMPE 2013 Conference and Exposition. 06-MAY-13, . : ,
09/01/2013	6.00	T. Tallman, K. W. Wang. Analytically modeling the piezoresistivity of CNT composites with low-filler aggregation, SPIE Smart Structures and Materials + Nondestructive Evaluation and Health Monitoring. 10-MAR-13, San Diego, California, USA. : ,
TOTAL:		**3**

Number of Peer-Reviewed Conference Proceeding publications (other than abstracts):

(d) Manuscripts

Received		Paper
TOTAL:		

Number of Manuscripts:

Books

Received		Paper
TOTAL:		

Patents Submitted

Patents Awarded

Awards

C. Bakis: Vice President, American Society for Composites, 2012 and 2013; President 2014 and 2015.

K.W. Wang: Distinguished Seminar Series Speaker, MAE Department 20th Anniversary Distinguished Seminar Series, Chinese University of Hong Kong, Hong Kong, China, January 2014; Plenary Speaker, Smart Materials and Structures Workshop, Harbin Institute of Technology, Harbin, China, January 2014.

Graduate Students

NAME	PERCENT_SUPPORTED	Discipline
Sila Gungor	0.25	
Tyler Tallman	0.25	
FTE Equivalent:	**0.50**	
Total Number:	**2**	

Names of Post Doctorates

NAME	PERCENT_SUPPORTED
FTE Equivalent:	
Total Number:	

Names of Faculty Supported

NAME	PERCENT_SUPPORTED	National Academy Member
Charles E. Bakis	0.02	
Kon-Well Wang	0.02	
FTE Equivalent:	**0.04**	
Total Number:	**2**	

Names of Under Graduate students supported

NAME	PERCENT_SUPPORTED
FTE Equivalent:	
Total Number:	

Student Metrics

This section only applies to graduating undergraduates supported by this agreement in this reporting period

The number of undergraduates funded by this agreement who graduated during this period: 0.00

The number of undergraduates funded by this agreement who graduated during this period with a degree in science, mathematics, engineering, or technology fields:..... 0.00

The number of undergraduates funded by your agreement who graduated during this period and will continue to pursue a graduate or Ph.D. degree in science, mathematics, engineering, or technology fields:..... 0.00

Number of graduating undergraduates who achieved a 3.5 GPA to 4.0 (4.0 max scale):..... 0.00

Number of graduating undergraduates funded by a DoD funded Center of Excellence grant for Education, Research and Engineering:..... 0.00

The number of undergraduates funded by your agreement who graduated during this period and intend to work for the Department of Defense 0.00

The number of undergraduates funded by your agreement who graduated during this period and will receive scholarships or fellowships for further studies in science, mathematics, engineering or technology fields:..... 0.00

Names of Personnel receiving masters degrees

NAME

Total Number:

Names of personnel receiving PHDs

NAME
Sila Gungor
Total Number: **1**

Names of other research staff

NAME PERCENT_SUPPORTED

FTE Equivalent:
Total Number:

Sub Contractors (DD882)

Inventions (DD882)

Scientific Progress

See attachment

Technology Transfer

Final Report

Novel Structural Health Monitoring Schemes for Glass-Fiber Composites using Nanofillers

Proposal No. 58085EG
Agreement No. W911NF-10-1-00267

Date of Report: 31 March 2014

Period of Performance: 1 Oct. 2010 to 31 Dec. 2013

Charles E. Bakis, Department of Engineering Science & Mechanics, Penn State University, University Park, PA 16802

Kon-Well Wang, Department of Mechanical Engineering, University of Michigan, Ann Arbor, MI 48109

Abstract

The objective of the investigation is to explore a new approach for high sensitivity structural health monitoring of continuous glass fiber reinforced polymer composites (GFRPs). Conductive nanofillers were used for tailoring the anisotropic conductivity of GFRP. Carbon nanotubes and carbon blacks were anisotropically networked using dielectrophoretic manipulation during processing. Smaller, low-aspect-ratio nanofillers (carbon black) in low concentrations were superior to high-aspect-ratio nanofillers (nanotubes) for electrical tailoring purposes. Networking of carbon black nanoparticles through the thickness increased the detectability of delamination. Electrical impedance tomography (EIT) was shown to be able to accurately locate through-hole damage as small as 3.18 mm in diameter as well as impact damage to a GFRP laminate with aligned carbon black. EIT has also been used to locate damage in a carbon nanofiber (CNF) filled epoxy composite. Methods of improving EIT for structural health monitoring of nanocomposites have been investigated. Experimentally, utilizing the conductivity evolution of CNF/epoxy for baseline free damage detection has been explored. Analytically, it has been shown that piezoresistive coupling and nanofiller alignment both enhance the ability of EIT to detect damage.

Table of Contents

1. Research Objectives

The objectives of this investigation are to explore a ground breaking approach for high sensitivity structural health monitoring of continuous glass fiber reinforced polymer composites via a two-pronged strategy:

- Investigate the use of conductive nanofillers for tailoring the anisotropic conductivity of continuous glass fiber reinforced composites, thereby increasing the sensitivity of electrical measurements to the size and orientation of damage
- Investigate algorithms to further enhance sensitivity and locate damage and quantify its extent with unprecedented sensitivity.

These objectives go well beyond currently known damage detection techniques based on the insertion of randomly oriented nanofillers and the monitoring of AC or DC electrical properties of continuous fiber composites. A secondary benefit of adding nanofillers to the matrix material of composites is the reduction of susceptibility to matrix damage such as intralaminar matrix cracks and delamination cracks.

2. Approach

This research aims to explore new ideas and research directions that will advance the state of the art:

- Apply electrical tailoring techniques to create glass fiber reinforced polymer (GFRP) composites with well-aligned carbon black (CB) or carbon nanotube (CNT) fillers and tailored anisotropic electrical properties for unprecedented sensitivity to matrix damage.
- Investigate non-intrusive, strain-compatible, durable carbon fiber electrodes for distributing the electrical sensing capability over a broad region of a composite panel to obtain improved sensing capability and reliability.
- Experimentally and analytically investigate the effect of aligned carbon black or CNT fillers on the electrical behavior of GFRP composites.
- Use the validated analysis to guide the improvement of SHM capability for GFRP composites using tailored anisotropic electrical properties.
- Improve damage detection sensitivity and location determination accuracy by leveraging unique properties of nanocomposites.
- Develop electrical impedance tomography into a robust damage tracking method for conductive composites.

3. Significance

Glass fiber composites have broad applicability in Army field applications, particularly ballistic armor and helicopter blades. The ability to detect matrix damage in composite laminates is extremely important because matrix damage can lead to stiffness reduction, fiber fracture and delamination-related compressive strength reduction.

This research complements related research on nanocomposites being carried out at Penn State with funding from National Science Foundation, Vertical Lift Consortium, and the National Rotorcraft Technology Center through the Vertical Lift Research Centers of Excellence program. The investigation could therefore be of interest to various Army laboratories. This research also complements related research on structural health monitoring being carried out at the University of Michigan with funding from the Air Force Office of Scientific Research.

4. Accomplishments

4.1. Evaluation of Nanofillers and Processing Methods for Tailoring the DC Conductivity of Epoxy Matrix

Carbon nanofiller/epoxy composites were manufactured to determine the effects of type of nanofiller, processing conditions, and electrical field parameters during processing on the electrical conductivity. Two types of specimens were fabricated for this purpose: (*i*) thin film specimens with high optical transparency (approximately 20 mm long × 5 mm wide × 0.16 mm thick); and (*ii*) bulk specimens (approximately 12 mm long × 12 mm wide × 10 mm thick). Thin film specimens offer suitable optical transparency for observing the morphology of nanofiller networks with an optical microscope. The bulk specimens allow the electrical resistivity to be easily measured parallel and transverse to the alignment direction. Throughout the investigation, an epoxy system consisting of 100 parts bisphenol-A based epoxide diluted with an alkyl glycidyl ether, EPON™ 8132, and 40 parts polyether amine curing agent, Jeffamine T403, was utilized.

4.1.1. Nanofiller Surface Functionalization and Aspect Ratio

Fillers with different aspect ratios, including long and short carbon nanotubes (CNTs), carbon nanofibers (CNFs), and carbon black (CB) were investigated to determine which are best for forming electrical networks within the epoxy by applying an AC electric field (dielectrophoresis) prior to gelation (Zhu, 2011). Some of the CNTs were functionalized by oxidation or by oxidation plus the addition of (3-glycidyloxypropyl)trimethoxysilane (GPS) coupling agent. For the unfunctionalized fillers, a nonionic surfactant named Triton X-100 ($C_{28}H_{53}O_9$) was added to the mixture at the same weight as the nanofiller to assist in dispersion. Figure 1 shows a comparison of resistivities along the networking direction and a photograph of networked CNTs between a pair of electrodes. The measurements indicate that surface functionalization significantly increases resistivity. This effect may be due to a more effective dispersion (electrical isolation) of functionalized CNTs and CNFs in the nonconductive matrix, a smaller length/diameter ratio of these particles due to functionalization, or a disruption of conductive paths within individual CNFs and CNTs due to functionalization, as observed previously by others (e.g., Wichmann et al. 2006). The fillers highlighted with arrows in Figure 1 are those considered best-suited for tuning electrical conductivity by virtue of their low resistivity upon network formation. Higher magnification micrographs of network morphologies for a few different nanofillers are shown in Figure 2.

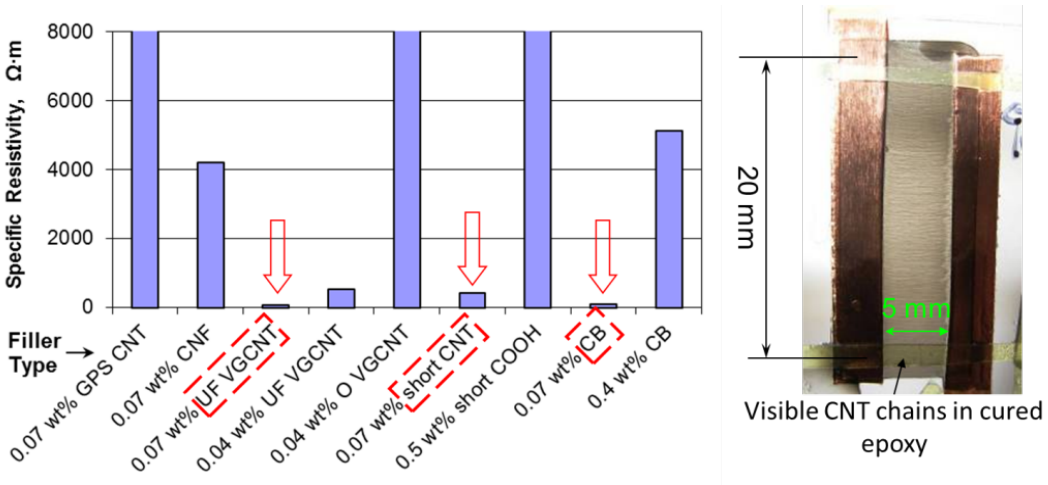

Figure 1. Resistivity of epoxy resin modified with different types of fillers including, GPS functionalized carbon nanotubes (CNTs), carbon nanofibers (CNFs), unfunctionalized vertical grown CNTs (UF VGCNTs), oxidized vertical grown CNTs (O VGCNT), short unfunctionalized CNTs (short CNT), short COOH functionalized CNTs (short COOH), and carbon black (CB), aligned with AC electric field at 1 kHz and 500 V/cm. Results obtained from thin film specimens. Weight percentages (wt%) shown are filler weight in percentage of epoxy resin weight.

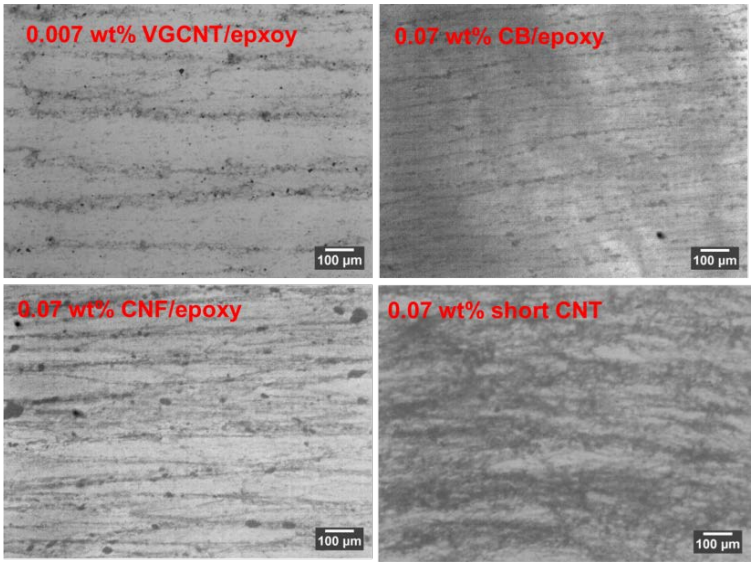

Figure 2. Optical microscope images showing morphology of nanofiller networks in cured epoxy. Specimens were made with the application of AC electric field at 1 Hz and 400 V/cm in the horizontal direction.

4.1.2. Sonication Dispersion Time, Amount of Surfactant, and Filler Concentration

The effects of sonication time and amount of Triton-X100 nonionic surfactant were determined using 0.05 wt% long CNT-filled epoxy by applying different durations of sonication and surfactant weights from 1 to 10 times that of the CNTs. The resulting resistivities of CNT/epoxy samples shown in Figure 3 indicate that while increasing sonication time did not affect the resistivity of unaligned CNT/epoxy specimens, it

decreases the resistivity of AC electric-field-aligned materials. It is concluded that a more conductive network can be obtained from longer sonication times. Since evidence suggests that longer sonication times reduce the length of CNTs by mechanical loading, a likely explanation for this result is that CNTs of low aspect ratio are more readily dispersed and preferentially networked by dielectrophoresis, compared to high aspect ratio CNTs (Zhu, 2011).

The effect of the nanofiller concentration was evaluated using short CNTs (Figure 4). With the application of electric field, the highest anisotropy ratio (electrical conductivity in the alignment direction divided by the transverse direction of) of ~75 was obtained at the lowest CNT concentration investigated (0.01 wt%). Also, a CNT concentration of about 0.1 wt% provided the lowest resistivity of all concentrations investigated. These results point to a need to trade-off low resistivity against high electrical anisotropy when tailoring the electrical properties of composites.

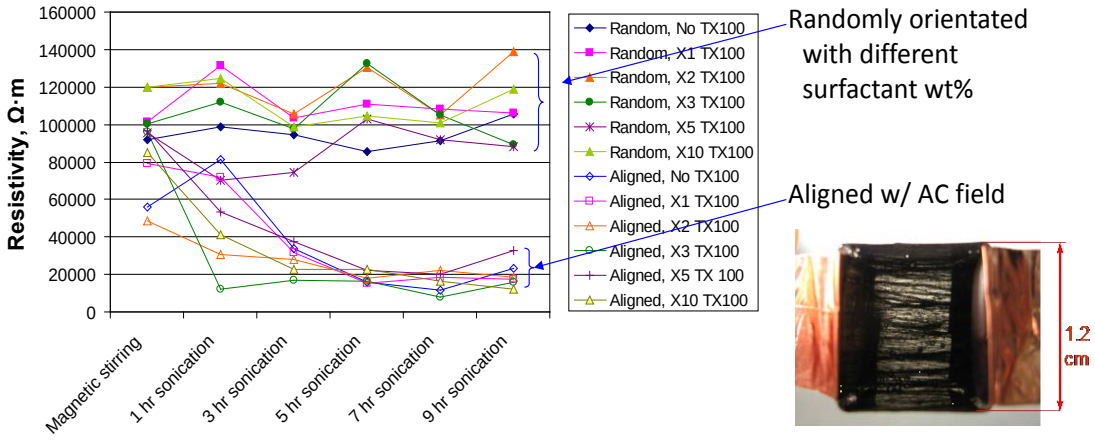

Figure 3. Resistivity of 0.05 wt% long CNT/epoxy processed by sonication. Sonication time ranged from 0 to 9 hours and surfactant weight from 1 to 10 times that of CNTs, with and without application of electric field during sample fabrication. (or aligned CNT/epoxy samples, AC electric field at 1 kHz and 400 V/cm was used.

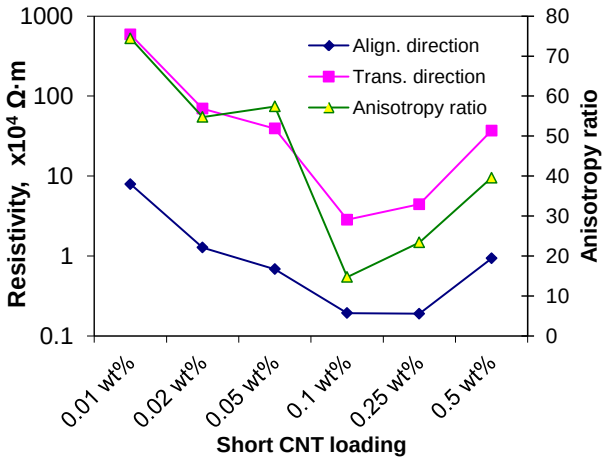

Figure 4. Resistivity of short CNT/epoxy specimens along the alignment direction and transverse to alignment direction. Samples were made using short CNTs, with an AC electric field applied at 1 kHz and 250 V/cm up till full cure.

4.1.3. Carbon Black

Carbon black is considered an interesting nanomaterial for tailoring the conductivity of fiber reinforced composites on account of its small size in relation to the length of other conductive particles such as carbon nanotubes. To observe the effects of different CB types, the following samples were procured from Cabot Corporation: Vulcan XC72, Vulcan XC605, and BlackPearls 2000. Vulcan XC72 was chosen due to its excellent electrical conductivity, whereas Vulcan XC605 grade was chosen due to its superior dispersability. Black Pearls 2000 grade was chosen due to its extremely high structure and surface area, as well as very fine particle size. Compared to low structure CBs, higher structure CBs tend to produce more conductive polymer composites (Rubin et al., 1999; Balberg, 2002). A 0.5 wt% CB concentration in the epoxide/curative mixture was selected for all types.

The CB particles were first mixed and stirred in 3.5 g of epoxide by using a magnetic stirrer operating at 300 rpm for 10 minutes. The CB concentration before adding the curative was 0.7 wt%. Following stirring, the mixture was sonicated at 45 kHz and 55 W for up to 10 hours. At one-hour intervals during sonication, the mixture was stirred with the magnetic stirrer at 300 rpm and small samples were placed on glass slides for inspection of the state of dispersion using an optical microscope. The optimum amount of sonication time was chosen for each material depending on the state of dispersion. The state of dispersion for each CB is given in Figure 5 for sonication times of 1 hour as well as the optimum time for each CB. For Vulcan XC72 and XC605 grades, there was not a significant change in the dispersion characteristics after 2 hours of sonication. Vulcan XC605 exhibited the most dispersed structure among all CB grades. The extremely high structure of BlackPearls 2000 can be clearly seen from Figure 5. Due to this property, it was not possible to have a good dispersion of this CB. The state of dispersion of BlackPearls 2000 was very similar for all sonication intervals and therefore a sonication time of 4 hours was arbitrarily chosen to be the “optimum.”

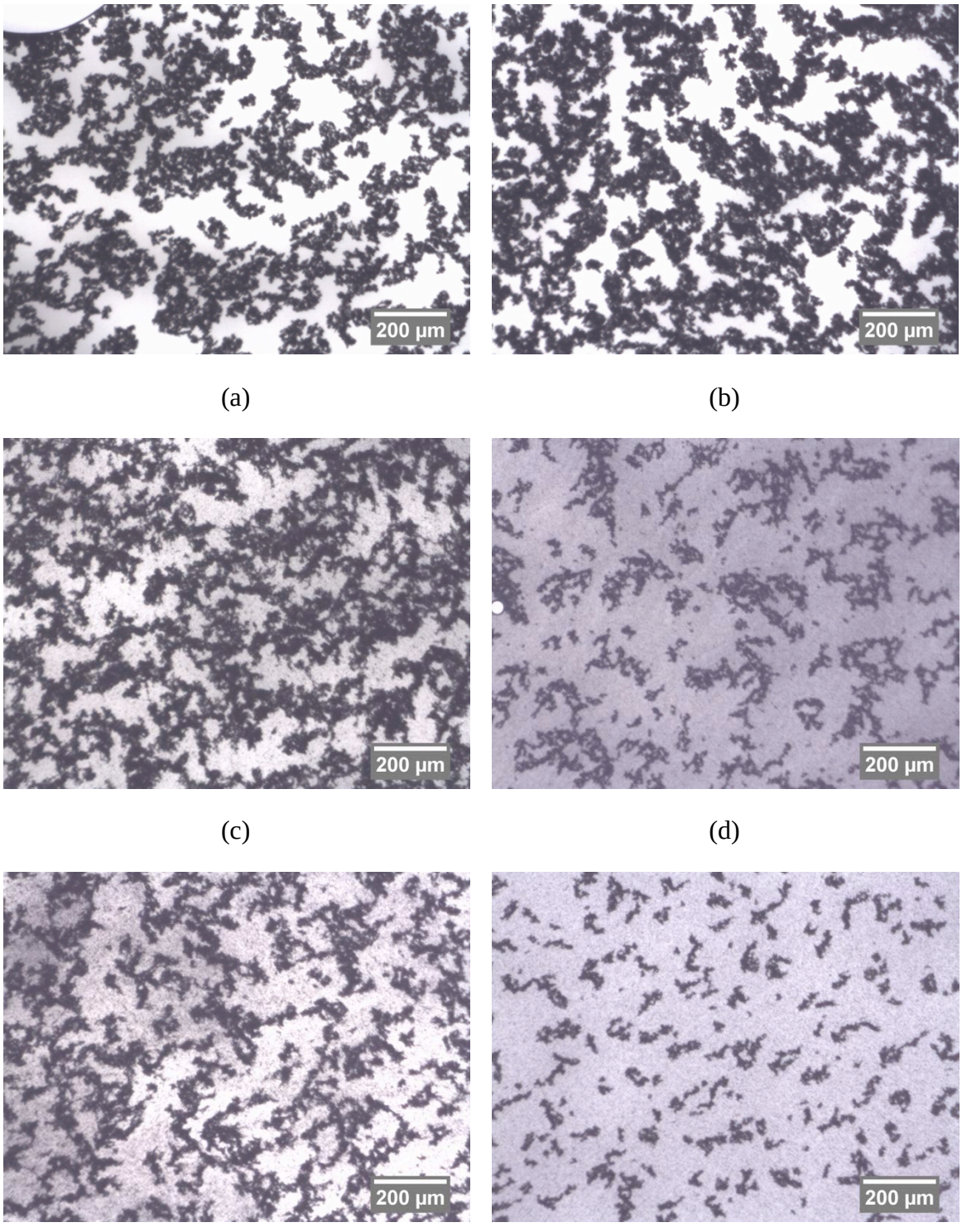

Figure 5. Optical micrographs of 0.7 wt% CB sonicated for various times in epoxide: (a) BlackPearls 2000 at 1 hr; (b) BlackPearls 2000 at 4 hr; (c) Vulcan XC72 at 1 hr; (d) Vulcan XC72 at 2 hr; (e) Vulcan XC605 at 1 hr; (f) Vulcan XC605 at 2 hr.

After the optimum sonication time was determined for each CB, thin films of networked and random CB/epoxy composites were produced to visually observe the morphology of CB particles and to compare the electrical conductivities of the materials following cure. Following the sonication of CB/epoxide mixtures, curing agent was added into the mixture. As mentioned before, the CB concentration in the epoxide/curative mixture is 0.5 wt%. The mixture was stirred by hand for 5 minutes to ensure the complete mixing of epoxide and curing agent, and was degassed for 30 minutes to eliminate most of the air bubbles. Two pieces of copper tape were placed on a glass slide with a 5 mm gap in between them. Following this, a glass cover was put on the copper tapes and the CB/epoxy mixture was injected in to the gap between the glass cover and the glass slide. An AC electric field of 800 V/cm strength and 1 kHz frequency was used during the production of networked CB/epoxy composites, whereas no electric field was applied during the production of random composites. The 5×22×0.16 mm films were cured on a hot plate.

DC conductivities of aligned and random configurations for each CB grade are given in Figure 6. As seen, for Vulcan XC72 and XC605 grades, there is almost a factor of 50 increase in the DC conductivity with the application of electric field. This behavior is attributed to the networking of CB particles along the electric field direction, which can be seen in Figure 7. For BlackPearls 2000, DC conductivity only increased by a factor of 15 with the electric field. Moreover, it was not possible to observe the chain formation in BlackPearls 2000/epoxy thin films. This is attributed to the high structure of this type of CB, which made it extremely hard to distinguish the CB chains. Although the chains in BlackPearls 2000/epoxy thin films could not be observed, the increase in the conductivity with the application of electric field points to a degree of networking. The highest conductivity was obtained in BlackPearls 2000/epoxy thin films, and therefore this type of CB was chosen to be used to manufacture the glass/epoxy composites discussed in next sections.

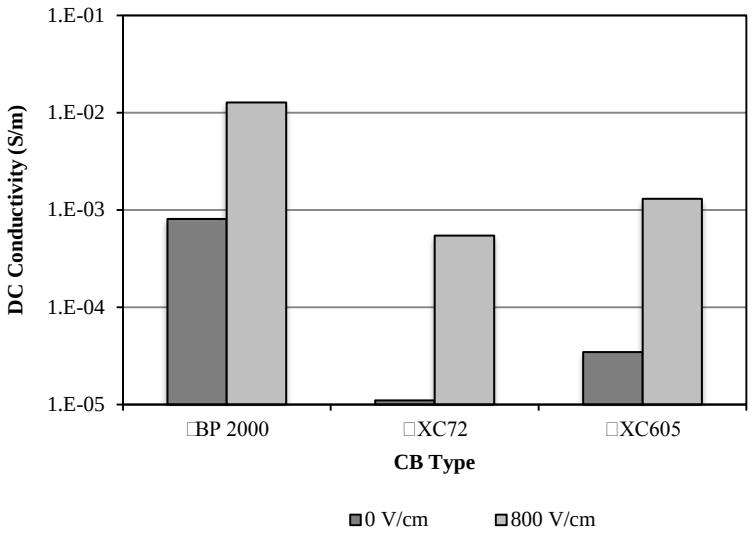

Figure 6. DC conductivity of random and aligned CB/epoxy composites with 0.5 wt% concentration in the epoxide/curative mixture. Alignment was done with 800 V/cm strength and 1 kHz frequency AC electric field.

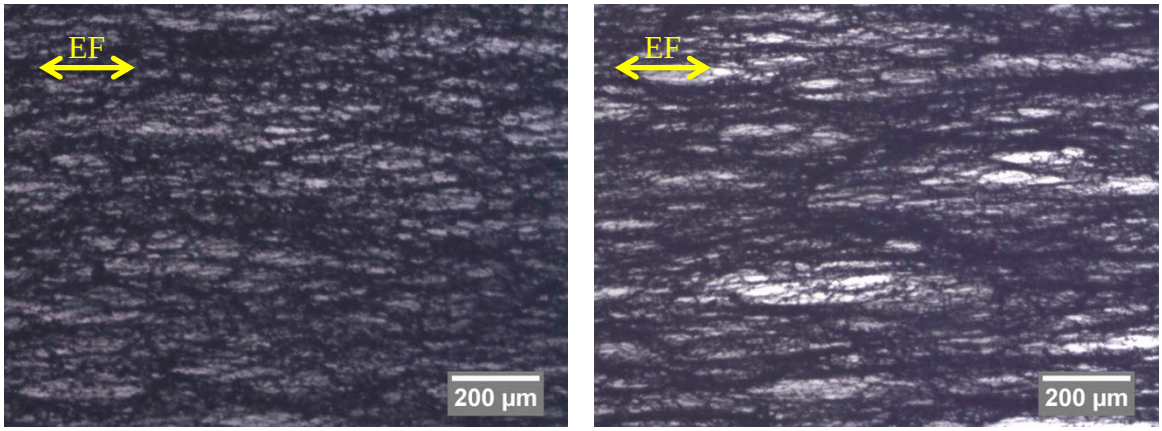

(a) (b)

Figure 7. Morphology of aligned CB chains formed using 800 V/cm, 1 kHz AC electric field and 0.5 wt% CB in the epoxide/curative mixture: (a) Vulcan XC72 CB; (b) Vulcan XC605 CB. The EF marker signifies the electric field direction.

4.1.4. Short Carbon Nanotubes

As a comparison to CB, the effects of CNTs on the electrical conductivity of epoxy and glass/epoxy composites were investigated. For this purpose, short, unfunctionalized, multiwalled CNTs were chosen as the candidate material due to their low aspect ratio, which is believed to ease their motion in between the densely packed glass fibers (Zhu, 2011). The manufacturer specifies the as-received length of the short CNTs as 0.5-2.0 µm and the outer diameter as 10-20 nm (i.e., length/diam. ratio of 25-200).

Based on the work described in Section 4.1.2, dispersion studies were carried out by using a target concentration of 0.1 wt% short CNTs in the epoxide/curative mixture,

which converts to 0.14 wt% in just the epoxide. The same epoxy resin system mentioned in Section 4.1.3 was used. In order to see the effects of surfactants on the dispersion characteristics of short CNT/epoxy mixture, a non-ionic surfactant, Triton X-100 (TX-100), was added into the mixture with a weight equal to 76% of the weight of short CNTs. The same dispersion procedure and sampling explained in Section 4.1.3 was used.

The optimum dispersion state was obtained when the materials were sonicated for 9 hours. The dispersion states of each material after 1 hour and 9 hours of sonication are given in Figure 8. It was observed that the use of Triton X-100 enhances the state of dispersion.

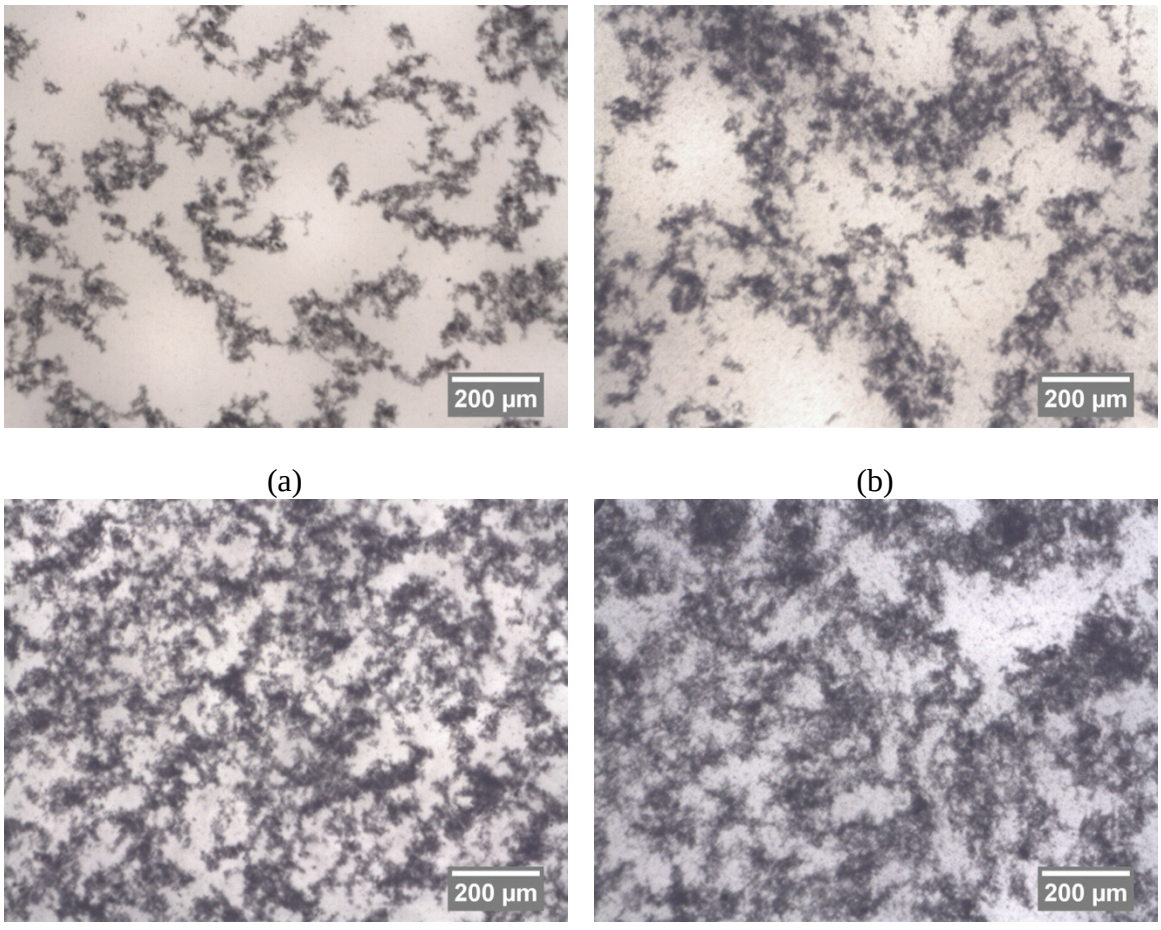

Figure 8. Optical micrographs of 0.14 wt% short, multiwalled, unfunctionalized CNTs sonicated for various times in epoxide: (a) 1 hour w/o Triton X-100; (b) 9 hours w/o Triton X-100; (c) 1 hour w/ Triton X-100; (d) 9 hours w/ Triton X-100.

In order to see the effect of dispersion on the electrical properties of short CNT/epoxy composites, thin films of short CNT/epoxide/curative mixture were processed with and without electric field. The electrical conductivities of the cured materials are presented in Figure 9. As shown, a roughly 50-fold increase in conductivity results from the application of an AC electric field for all of the materials. It is further observed that the

amount of sonication does not significantly change the electrical conductivity of short CNT/epoxy composites. Although TX-100 enhances the dispersion state, it does not have a significant influence on the electrical conductivity. These observations hold for both aligned and random specimens. In all of the aligned specimens, CNT chains were observed, as shown in Figure 10.

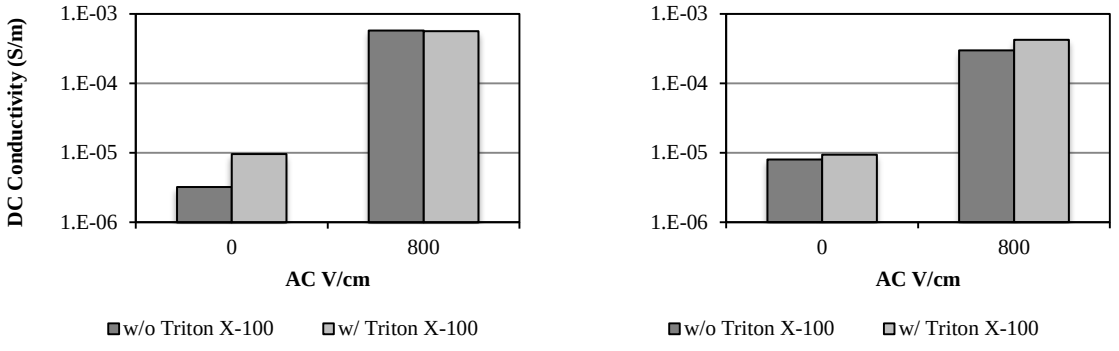

(a) (b)

Figure 9. DC conductivities of cured epoxy containing aligned and random short CNTs at 0.1 wt% concentration. Alignment was done with 800 V/cm strength and 1 kHz frequency AC electric field: (a) 1 hr sonication; (b) 9 hr sonication.

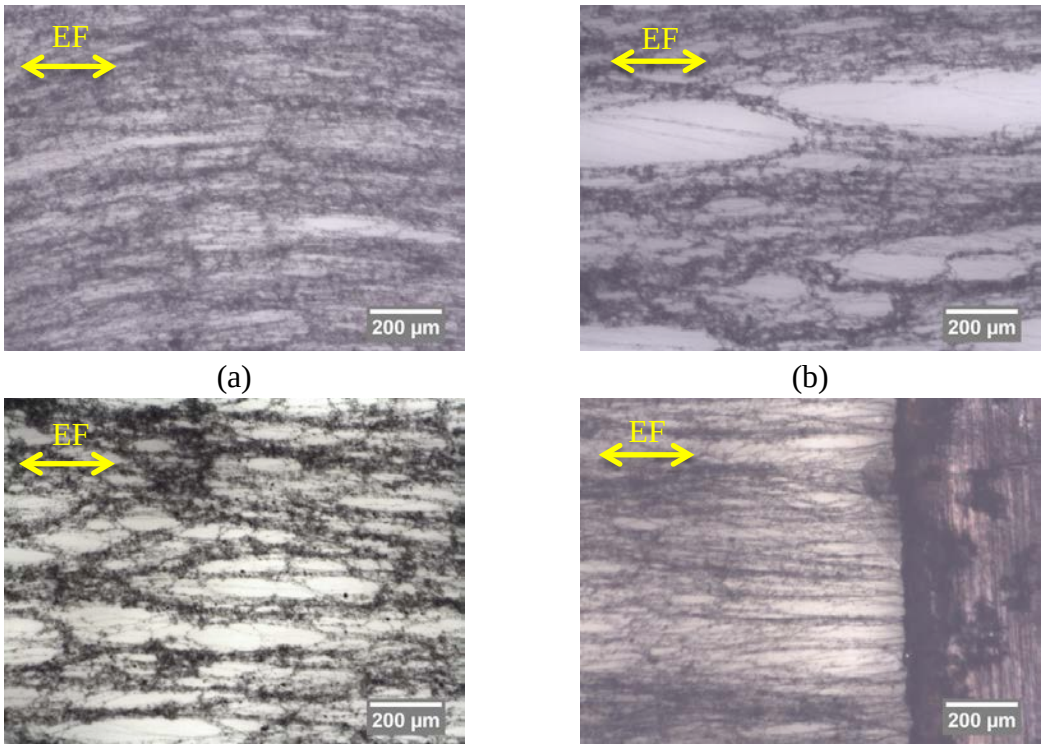

Figure 10. Morphology of aligned short CNT chains formed using 800 V/cm, 1 kHz AC electric field and 0.1 wt% CNTs in the epoxide/curative mixture: (a) 1 hr sonication w/o Triton X-100; (b) 9 hr sonication w/o Triton X-100; (c) 1 hr sonication w/ Triton X-100; and (d) 9 hr sonication w/ Triton X-100. The EF marker signifies the electric field direction.

4.2. Evaluation of Nanofiller Concentration and Electric Field Parameters for Tailoring the DC Conductivity of Unidirectional Glass/Epoxy Composites

4.2.1. Carbon Black Concentration

Carbon black (CB) was used as the baseline conductive filler in unidirectionally (UD) reinforced glass/epoxy composites due to its low aspect ratio, which is a promising feature for enabling the movement of CBs along and through the glass fibers that will result in preferential conductive network formation (Zhu, 2011). Different amounts of CB and alignment field strength were used to observe their effects on the DC electrical anisotropy of UD composites. CB nanofillers were dispersed in epoxide by sonication for 4 hours. Subsequently, curative was added. Composite plates with dimensions of 50 mm length × 50 mm width × 2.5 mm thickness were produced by hand layup and vacuum bagging using UD stitched E-glass fibers and dispersed CB-filled epoxy resin. The fiber volume fraction is estimated as 59-60% based on cured ply thickness and fiber areal weight measurements. The vacuum bag arrangement is shown in Figure 11. Aluminum foil electrodes were used on the top and the bottom of the composite plate for the networking of CB through the thickness prior to cure. After the application of vacuum, AC electric field was applied to the part and kept on during the whole curing cycle.

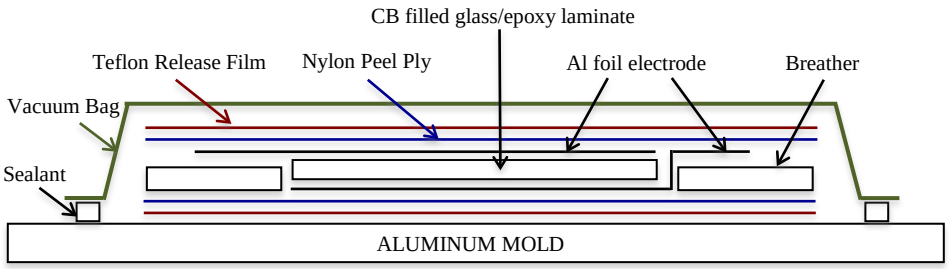

Figure 11. Cross-section view of the vacuum bag for manufacturing CB-filled glass/epoxy composites.

Cured composite plates were cut into a smaller dimension of 30×30×2.5 mm for resistance measurements. The aluminum foil alignment electrodes were removed and all surfaces were sanded. Silver paint was then applied to the parallel surfaces across which resistance was to be measured. The silver paint was removed and applied to two other opposite surfaces so that DC resistance could be measured in three different directions: through-thickness, in-plane longitudinal (relative the continuous glass fibers), and in-plane transverse. In order to measure the DC resistance, various DC voltages were applied to the cured parts and the corresponding DC currents were measured. DC resistance was calculated from the slope of the voltage-current graph. Figure 12 shows the effect of CB amount on DC conductivity of UD glass/epoxy composites with field of 800 V/cm AC voltage and 1 kHz applied through the thickness.

Figure 12 shows that there is an overall increase in the DC conductivity of UD glass/epoxy composites in all directions when the CB amount increases. The ratio of through-thickness conductivity to in-plane conductivities was highest for 0.5 wt% CB. Beyond 1.0 wt%, the change in conductivity is less significant, suggesting a stabilization of network formation beyond 1.0 wt% CB.

It is also seen that higher DC conductivities are consistently obtained along the in-plane direction, whereas the lowest conductivity is consistently obtained along the through-thickness direction. It can be expected that CB chains will form more readily in the in-plane directions since resin flow is predominantly in these directions during processing. For 0.3 wt% CB, in-plane longitudinal and transverse conductivities are very close to each other. It is further observed that as CB amount increases, in-plane longitudinal conductivity becomes greater than the in-plane transverse conductivity. In turn, in-plane longitudinal conductivity can be expected to be higher compared to in-plane transverse conductivity due to unhindered conductive pathways in the channels of resin parallel to the UD glass fibers, as observed by Thostenson et al., 2009 in the case of CNTs dispersed in UD glass FRP composites. The reproducibility of the results, shown in Figure 12 by error bars for certain cases, is such that the trends observed in these experiments can be considered significant.

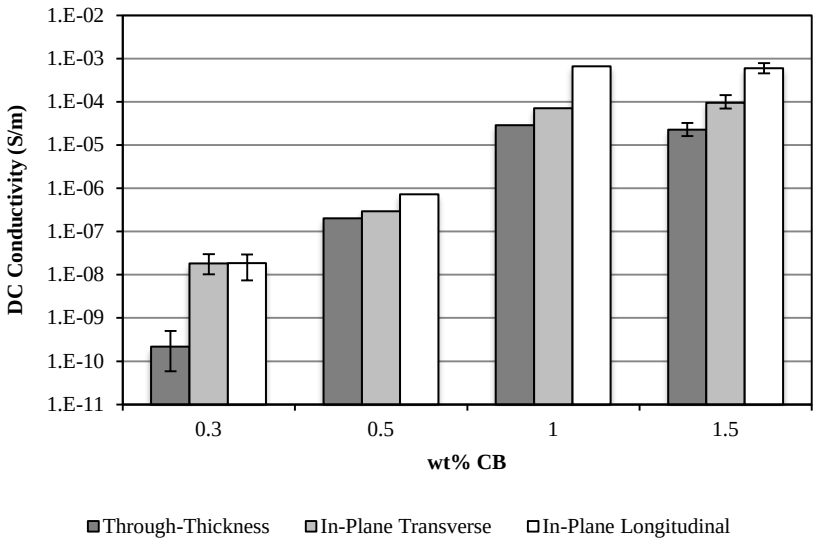

Figure 12. DC conductivities of glass/epoxy composite plates for different CB amounts. Peak-to-peak AC voltage - 800 V/cm, AC frequency - 1 kHz. Error bars indicate the maxima and the minima of three separate specimens prepared in an identical manner.

4.2.2. AC Voltage

In order to ascertain the effect of the magnitude of AC field during cure on final DC conductivity, 0.5 wt% CB filled UD E-glass/epoxy composites (manufactured as described in the previous section) were networked using different voltages. The conductivity results are shown in Figure 13. It was aimed to obtain higher conductivity in the through-thickness direction than in-plane directions. With increasing applied voltage, an increase in through-thickness and in-plane transverse conductivities was observed, with insignificant changes in the in-plane longitudinal conductivity. This suggests that the geometrical advantage of conductive pathways parallel to the fibers is difficult to overcome with an electric field applied perpendicular to the fibers. It is noteworthy that the in-plane transverse conductivity increases along with the through-thickness conductivity as alignment voltage increases. However, the in-plane transverse conductivity does not increase as much as the through-thickness conductivity. A certain degree of increase in the in-plane transverse conductivity can be expected due to: (a) flow of the resin in this direction during consolidation, as evidenced by the in-plane transverse conductivity being about 100 times greater than the through-thickness conductivity with no alignment voltage applied; and (b) a certain degree of networking of the CB chains in the in-plane transverse direction as the chains are forced to bend around the glass fibers. High in-plane longitudinal conductivity can be expected due to the collimated paths of conductive matrix material parallel to the fibers. For 0.5 wt% CB filled UD glass/epoxy composites aligned at 800 V/cm, 1200 V/cm and 1600 V/cm with 1 kHz frequency, conductivity in through-thickness direction became very close to the conductivities in in-plane directions, which should prove to be beneficial for the superior detection of delamination type flaws in the composite plate by electrical resistance-based techniques.

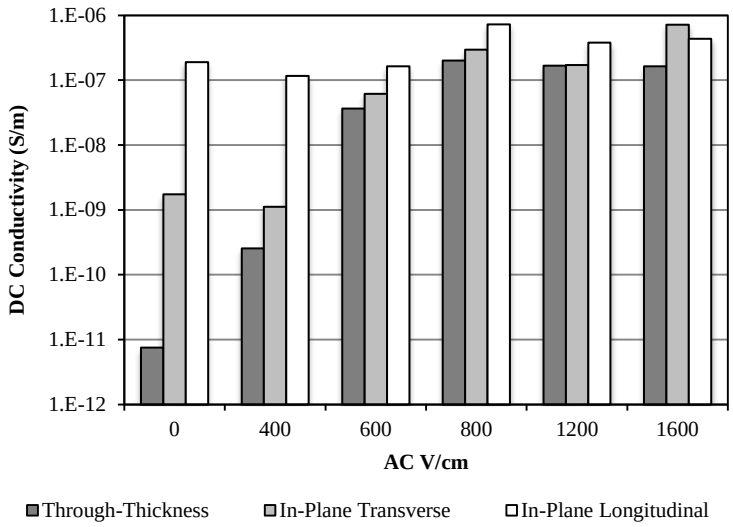

Figure 13. DC conductivities of 0.5 wt% CB-filled glass/epoxy composite plates for different peak-to-peak AC voltages (1 kHz AC Frequency).

With no applied electric field, the conductivity in the through-thickness direction is less than that in the in-plane longitudinal direction by a factor of 10^4. With the application of electric field, this factor diminished to as small as 10^1 due to significant increases in through-thickness conductivity and relatively small changes in the in-plane longitudinal conductivity. For peak-to-peak AC voltages of 800 V/cm and greater, conductivities did not change additionally, suggesting a point of diminishing returns.

For the 0.5 wt% CB-filled glass-epoxy composite plate, the highest DC electrical conductivity along through-thickness direction was obtained when the applied voltage was 800 V/cm. For this case, through-thickness conductivity increased by a factor of 10^4 with respect to the case where no electric field is applied. The conductivity changes along in-plane directions were considerably smaller compared to through-thickness conductivity change. To the best knowledge, this is the first time such a high increase in through-thickness conductivity has been observed in UD glass-epoxy composites with conductive nanofillers. Previous investigations demonstrated about one order of magnitude increase in the through-thickness conductivity of glass FRP composites with CNT fillers by applying an AC electric field curing processing (Wichmann et al., 2006; Domingues et al., 2012).

The effect of AC voltage on glass FRP plates containing 1.0 wt% and 1.5 wt% CB was also investigated (Figure 14). For 1.0 wt% CB-filled glass-epoxy composites, there is a slight increase in the conductivities along each direction with an increase in alignment voltage. Although the increase is not as remarkable as the 0.5 wt% CB-filled glass-epoxy plates, the 1.0 wt% composition also gives a similar overall response to AC alignment voltage. However, this is not the case for 1.5 wt% CB composition. For the 1.5 wt% CB case, the conductivities in the three directions are relatively unaffected by the change in AC alignment voltage. This result suggests that there exists a composition beyond which conductivities do not respond to AC alignment voltage. This is attributed to the

immediate formation of a 3-dimensional network of fillers even before any AC field is applied. The applied field is then routed directly through the network, preventing the formation of preferentially aligned chains of CB.

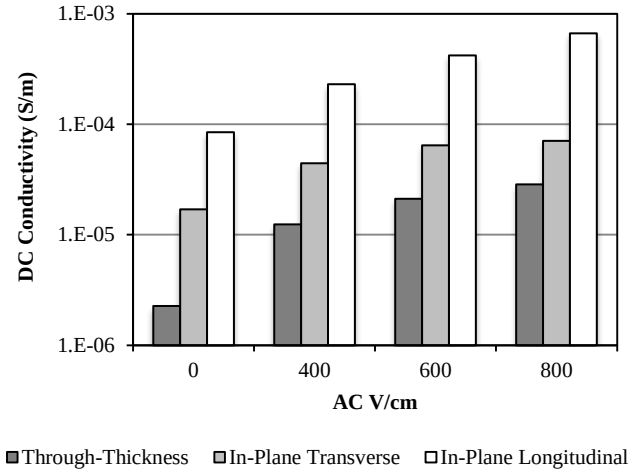

(a)

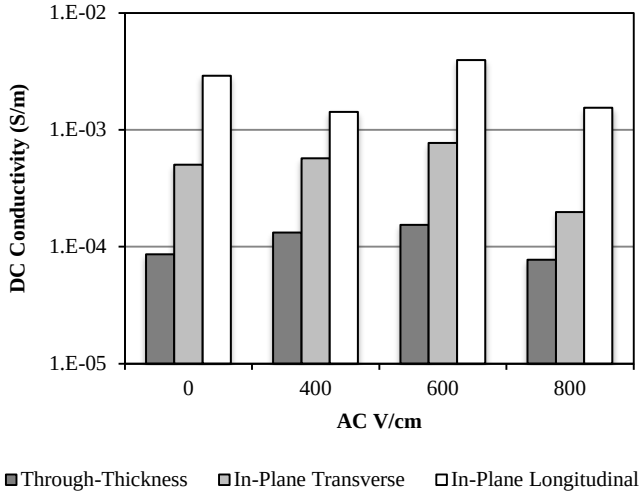

(b)

Figure 14. DC conductivities of (a) 1.0 wt%, (b) 1.5 wt% CB-filled glass/epoxy composite plates for different peak-to-peak AC voltages (1 kHz AC frequency).

4.2.3. AC Frequency

The effect of frequency on the chaining of CB in glass-epoxy composites was investigated for the 0.3 wt% CB composition and 1200 V/cm peak-to-peak AC voltage. These parameters were chosen based on their potential to maximize the ratio of through-thickness to in-plane conductivity (as discussed later). Three different frequencies were evaluated: 100 Hz, 1 kHz, and 10 kHz (Figure 15). It can be seen that the effect of

frequency is not as remarkable as the effect of voltage and CB amount. Although the frequencies were changed logarithmically, conductivity values did not vary considerably. Overall, these findings suggest that frequency does not have a significant effect on the preferential alignment of CB chains and, hence, DC conductivities in UD glass/epoxy composites for AC field strength of 1200 V/cm and 1 kHz frequency.

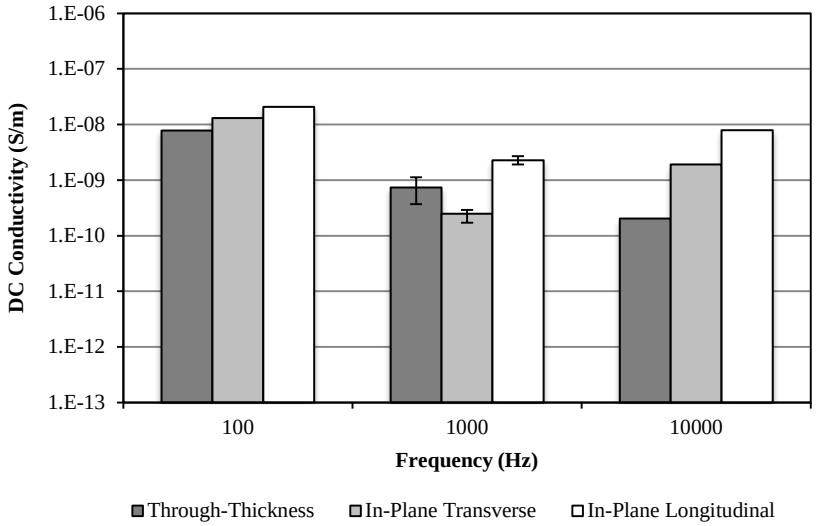

Figure 15. DC conductivities of 0.3 wt% CB-filled glass/epoxy composite plates over the frequency range (100 Hz to 10 kHz) investigated. Peak-to-peak AC voltage: 1200 V/cm. Error bars indicate the maxima and the minima.

4.2.4. Anisotropy Studies

The effects of CB amount, AC voltage and AC frequency on the conductivities of CB-filled glass/epoxy composite plates were investigated as described in previous sections. It was possible to enhance the through-thickness conductivity considerably by optimizing the mentioned parameters. In fact, it was enhanced in such a way that conductivity in through-thickness direction surpassed the conductivity along in-plane transverse direction. Figure 16 shows the two anisotropy ratios, defined as the ratio of through-thickness conductivity to in-plane transverse conductivity (σ_3/σ_2) and the ratio of through-thickness conductivity to in-plane longitudinal conductivity (σ_3/σ_1), for different compositions and electric field strengths. Both of the anisotropy ratios, namely σ_3/σ_2 and σ_3/σ_1, exhibited a similar behavior with σ_3/σ_2 being greater than σ_3/σ_1 for all the cases. Moreover, anisotropy ratio σ_3/σ_1 was less than 1 for all cases, whereas the anisotropy ratio σ_3/σ_2 exceeded 1 for some particular composition and processing parameters. For 1.0 wt%, and 1.5 wt% CB amounts, anisotropy ratio σ_3/σ_2 were well below 1. This is attributed to the immediate network saturation of CB chains in the 1.0 wt% and 1.5 wt% compositions. For 0.5 wt% CB and 1200 V/cm applied voltage, the anisotropy ratio σ_3/σ_2 approached 1. For 0.3 wt% CB at 1200 V/cm and 1600 V/cm, anisotropy ratios σ_3/σ_1 and σ_3/σ_2 were equal to 1.6 and 3.3, respectively. To the best knowledge of the authors, this is the first investigation where an anisotropy ratio greater than 1 was obtained in UD glass/epoxy composites. For this composition, it is believed that there were enough CB

particles to form continuous chains along through-thickness direction, yet not too much to lead to immediate network saturation, which may hinder particle movement and preferential chain formation.

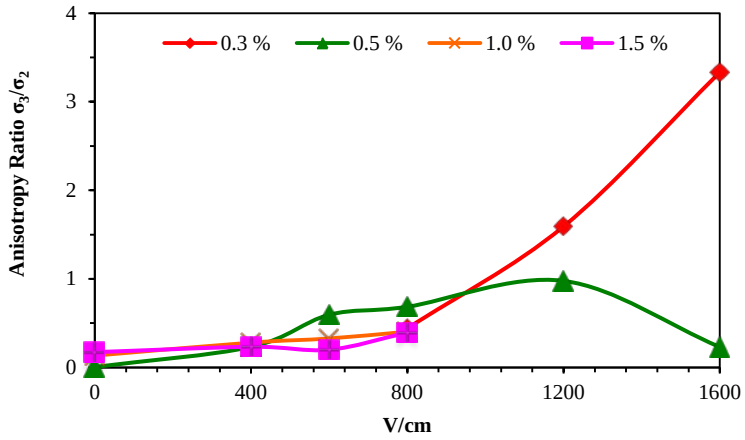

(a)

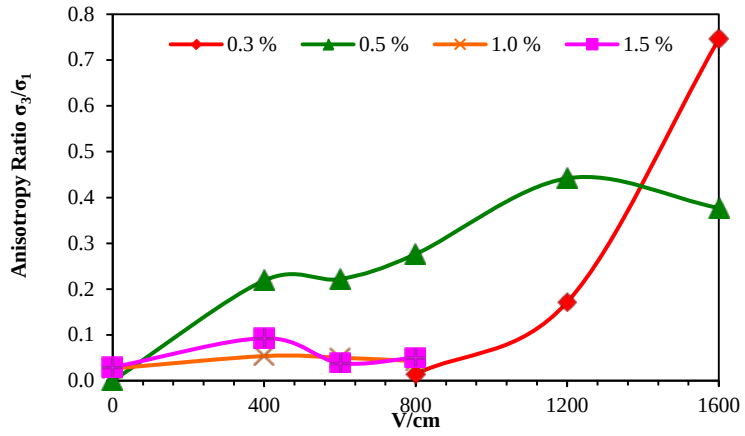

(b)

Figure 16. Anisotropy ratios (a) σ_3/σ_2, and (b) σ_3/σ_1 of glass-epoxy plates made with different weight percents of CB, with respect to AC voltage applied for alignment. AC frequency - 1 kHz. (σ_1 – In-plane longitudinal, σ_2 – In-plane transverse, σ_3 – Through-thickness conductivities)

4.2.5. Short Carbon Nanotubes

In order to determine the influence of CNTs on the conductivity of glass/epoxy composites, 0.1 wt% short CNT was dispersed into epoxy matrix material with the presence of Triton X-100 surfactant for 9 hr. Unidirectionally reinforced composite plates were produced by hand lay-up and vacuum bagging. For the sonication step, a short CNT/epoxide batch size of 7 g was used to manufacture the laminates. Eighteen layers of 225 g/m^2 E-glass were used. On the top and bottom surfaces of the laminates, aluminum foil was used as electrodes for aligning short CNTs. Electric field was applied during the

entire curing time. Based on the measured thickness of cured laminates, the glass fiber volume fraction of the composites is calculated to be 0.60±0.02. After curing, laminates were cut into a dimension of 30×30×2.5 mm by using a water-cooled diamond saw. Following the cutting procedure, aluminum foils were peeled off the top and bottom surfaces and the same surfaces were sanded by using 220, 400, 600 grit sandpapers in succession. The sanded surfaces were cleaned with acetone and silver paint was applied as an electrode material for measuring the DC conductivity along the thickness direction of the laminates. In order to measure the DC conductivity, a voltage versus current curve was constructed and resistance was calculated from the slope. An AC peak-to-peak voltage of 800 V/cm and 1 kHz frequency was used during the production of aligned short CNT filled glass/epoxy composites. Through-thickness DC conductivities of both random and aligned short CNT filled glass/epoxy composites were smaller than 10^{-11} S/m—the lower limit of the instrumentation used for measuring conductivity. To obtain higher conductivities, glass/epoxy composites with 0.3 wt% and 0.5 wt% short CNTs in the epoxide/curative mixture were also produced (Figure 17). As expected, higher conductivities were obtained when the short CNT amount was increased. However, for both of the cases, a significant increase in the conductivity was not obtained with the application of electric field. This is attributed to the high concentration of CNTs which produces larger agglomerates that cannot be aligned and chained within an array of densely packed glass fibers using an electric field.

In summary, when identical amounts of short CNT and CB are used in glass/epoxy composites (0.5 wt%), higher conductivities are obtained in aligned CB filled glass/epoxy composite than in CNT filled glass/epoxy composite. Moreover, electric field does not have a significant effect on the conductivity of CNT filled glass/epoxy composite, whereas it increases the conductivity of CB filled glass/epoxy composite by a factor of 10^3.

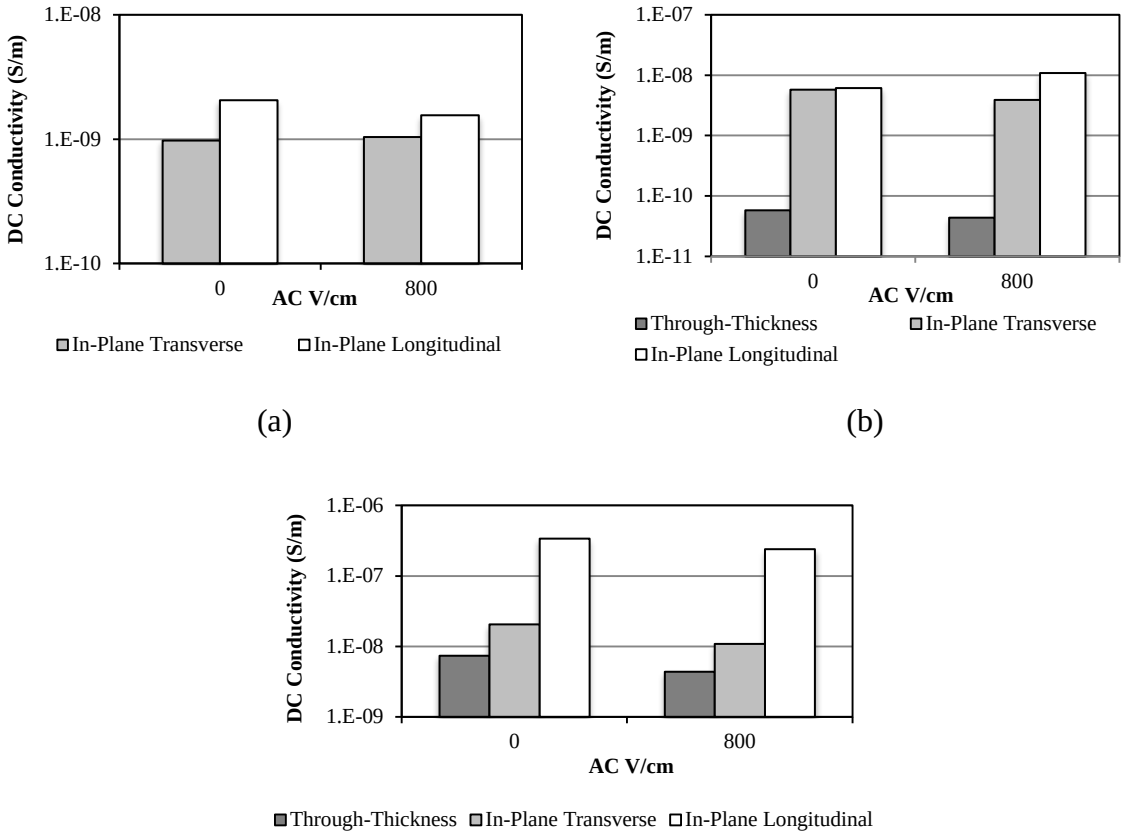

Figure 17. DC conductivity of random and aligned short CNT filled unidirectionally reinforced glass/epoxy composites having a calculated fiber volume fraction of 0.60±0.02 for (a) 0.1 wt%, (b) 0.3 wt%, and (c) 0.5 wt% short CNT composition. Alignment was done with 800 V/cm strength and 1 kHz frequency AC electric field.

4.3. Interlaminar Crack Sensing in Glass/CNT/Epoxy Composites using the DC Electrical Resistance Measurement Method and Rudimentary Electrode Configurations

Since laminated fiber reinforced polymer composites are susceptible to delamination and strength reduction due to impact damage, methods of detecting delamination on a continuous basis are of great interest. In the current investigation, in this section, the DC electric resistance monitoring method is employed with carbon nanotubes and nanofibers added to the liquid epoxy resin for conductivity and glass fiber used as the primary reinforcement. The objective is to maximize the sensitivity of electrical resistance measurements to delamination by tailoring the electrical conductivity of the composite during processing. It was analytically shown by Tallman et al. (2012) that the sensitivity for delamination detection increases with increasing ratio of through-thickness to in-plane conductivity. The conductivity in the through-thickness direction is increased by the application of an AC electric field to the nanofilled fiber preform, which promotes anisotropic chaining of the particles which is locked in place following cure. The

specimens described in this section were manufactured with rudimentary electrodes that cover the entire surface of the laminate—a configuration that allows damage growth during loading to be observed but prevents determination of the location of the damage in the laminate. The experiments in this section were completed before the experiments described in the previous sections showed that CB can be more readily aligned than CNTs and CNFs. Thus, only CNTs and CNFs were used. Additional details of the experiments described in this section can be found in Zhu (2011) and Zhu and Bakis (2012).

Interlaminar fracture specimens manufactured with unidirectionally reinforced glass fiber reinforced composites with aligned 0.125 wt% vertical grown CNT/epoxy (VGCNT) as the matrix were used to assess the ability of the electrical resistance method to detect mode I and mode II crack growth using a simple electrode arrangement. A flat plate was manufactured using the filament winding method to produce the pre-impregnated material. Fiber layers were wound circumferentially on a flat paddle mandrel and individually impregnated by manually applying pre-dispersed VGCNT/epoxy mixture at each interlayer using a roller. Each interlayer contained enough resin to impregnate one layer of dry fiber. Two 10-layer sheets of wet unidirectionally reinforced composite were removed from the mandrel and stacked in a silicone mold with a 12.7 μm thick PTFE film at the mid-plane of the 20-layer laminate to serve as a crack starter, as shown in Figure 18a. Aluminum films were applied on the top and bottom surface of the wet composite to serve as electrodes for aligning and chaining the nanofillers through the thickness during curing. Once the mold was placed into a programmable hot press, electric field was applied as soon as the mold pressure reached 240 kPa and was left on for the entire cure cycle. The AC field was initially set to 500 V/cm and 1 kHz. However, as the uncured material became more conductive during heating and nanofiller alignment, the field strength dropped to about 1/3-1/2 of the initial strength. The glass fiber volume content of the flat plate was 62% and the plate thickness was approximately 3.5 mm.

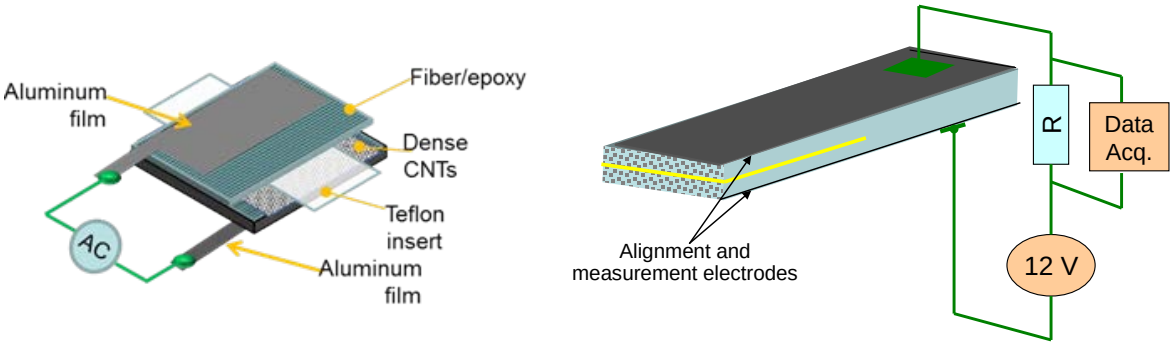

(a) (b)

Figure 18. Method of manufacture (a) and electrical test (b) of interlaminar fracture toughness specimens with 0.125 wt% VGCNT/epoxy.

Mode I double cantilever beam (DCB) and mode II end-notched-flexure (ENF) interlaminar fracture tests were conducted using standard specimens cut from the flat

plates (ASTM D5528-01, 2007; JIS K 7086, 1993). During the tests, DC electrical resistance of the specimens was measured using the aluminum films as the electrodes covering the top and bottom surfaces of the specimens, as shown in Figure 18b. Representative load versus displacement and resistance versus displacement curves are shown in Figure 19a for a mode I test and Figure 19b for a mode II test. It can be seen that the resistance changes in response to initiation of the crack growth, demonstrating that electrical measurements can detect delamination growth with good sensitivity by using CNT-filled epoxy resin.

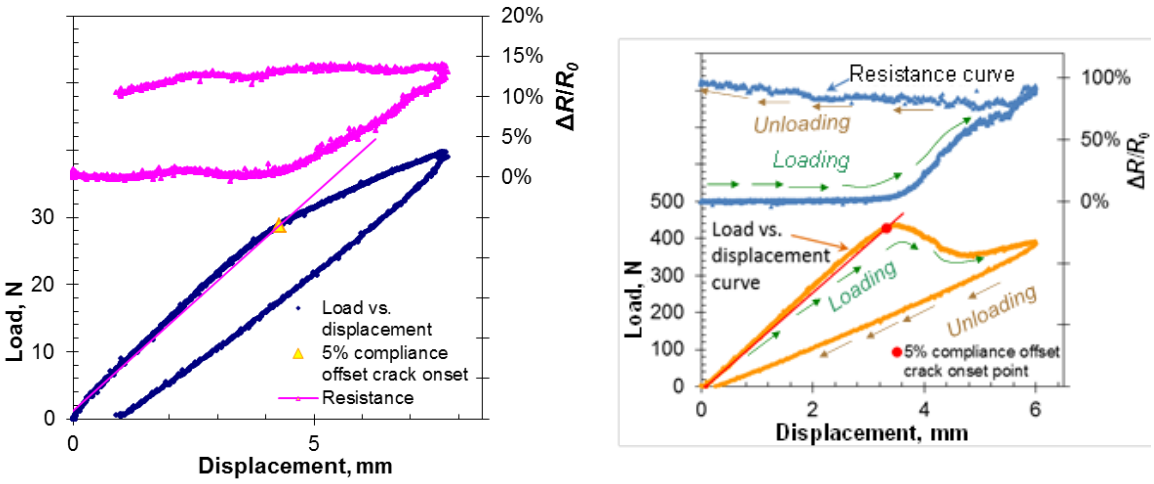

(a) (b)

Figure 19. Normalized resistance change and load versus load point displacement curves for a mode I DCB specimen (a) and a mode II ENF specimen (b) made with 0.125 wt% VGCNT/epoxy resin.

Glass fiber-reinforced composite cylindrical tubes made with aligned 1 wt% CNF/epoxy resin were also made for assessing the ability of the DC electrical resistance method to detect the growth of damage caused by quasi-static indentation. The tubes were manufactured by filament winding using the ply-by-ply, manual impregnation method described in the previous discussion for flat plates. A 48-mm-diameter aluminum mandrel was used. Aluminum foil was wrapped around the entire surface of the mandrel to serve as one of the alignment electrodes. A layer of dry fibers with the desired winding pattern was then wound using a programmable winder, as shown in Figure 20a. The dry ply was impregnated with pre-dispersed CNF/epoxy resin using a roller. After winding each of the five layers and interlayers to obtain a $[\pm 45/(\pm 2)_2/(\pm 45)_2]$ laminated tube (plies listed from inner diameter to outer diameter), aluminum foil was wrapped around the outer surface of the tube to serve as the second alignment electrode. A porous release tape was spirally wrapped with tension around the tube to absorb the excess resin. Release-coated shrink tape was wrapped around the release cloth to supply compaction pressure. AC electric field at 1 kHz was applied after placing the mandrel in the oven and was left on until the cure schedule was complete. Similar to the situation with plates, the electric field strength started at 500 V/cm and dropped to roughly 200 V/cm as the temperature of the material increased. After cure, the tubes were cut into specimens of 75 mm length

using a water-cooled abrasive saw. The tubes had an average wall thickness of 2.0 mm without the electrodes.

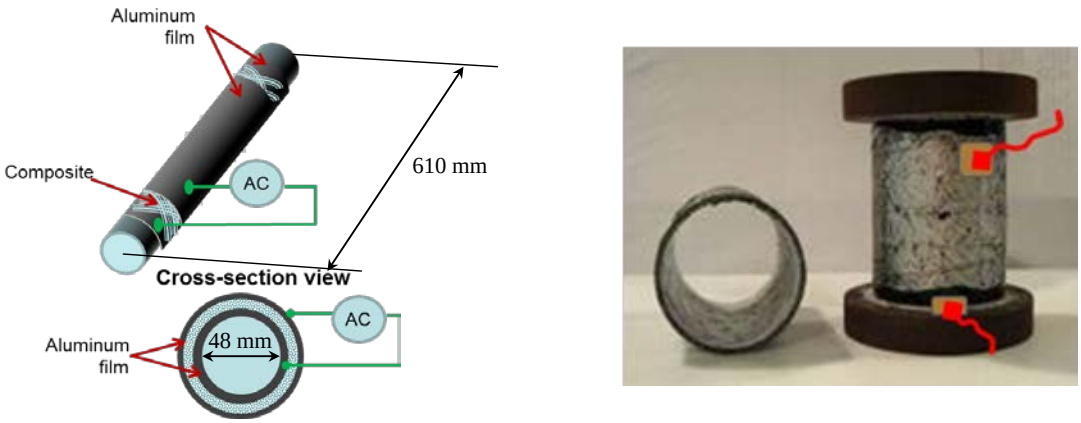

(a) (b)

Figure 20. Method of manufacture (a) and electrical test (b) of tubular GFRP specimens with 1 wt% CNF/epoxy. The red lines in (b) indicate wiring.

The circuit and connection method used for measuring resistance of tube specimens are fundamentally the same as those for the ILF specimens. Figure 20b shows the portions of the inner and outer surface covered with aluminum electrode material (silver colored regions). The entire inner surface of the tube is entirely covered by an electrode, while only the part of the outer surface away from the two ends is covered by the other electrode. A thin layer of epoxy was applied to the exposed portions of the tube for electrical insulation. These electrical details were designed to avoid a short circuit between the electrodes when the ends of the tube were potted into grooves in steel gripping fixtures with a conductive bismuth alloy. With this arrangement, one wire could be attached to any point on the outside electrode while the other could be attached to a point on the either gripping fixture for measuring through-thickness resistance of the tube. Tubes were quasi-statically indented as shown in Figure 21a and loaded to failure in axial compression while resistance was monitored, as shown in Figure 21b.

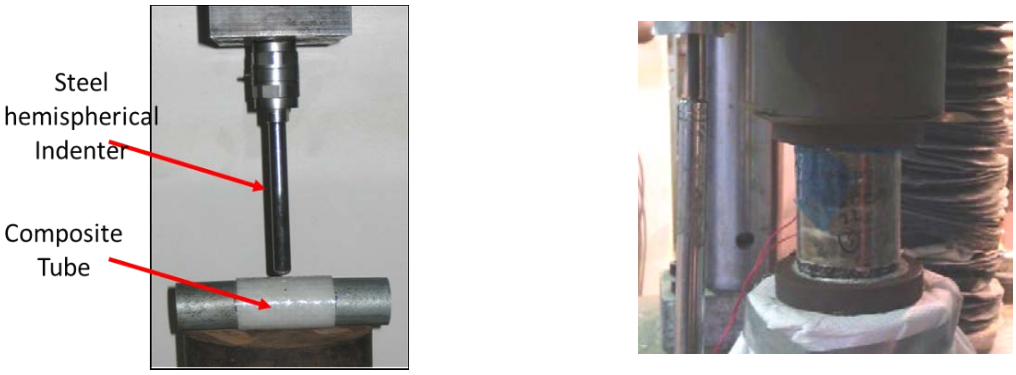

(a) (b)

Figure 21. Test setups for tubes: (a) quasi-static indentation (no nanofiller in tube shown); (b) compression-after-indentation.

Typical longitudinal stress versus strain and resistance versus strain curves for compression-after-indentation tests on indented tubes are shown in Figure 22. After the longitudinal strain (crosshead displacement divided by gage length) reached about 15 mm/m, the resistance increased slightly, possibly due to propagation of damage caused by indentation. Failure of the specimen coincided with a rapid 30% increase in resistance. Even after unloading, a roughly 30% increase in resistance can be seen, indicating that the DC electrical resistance method provides a permanent record of damage growth. To the knowledge of the authors, this is the first use of tailored nanofiller to detect damage in filament wound GFRP composites using the ER technique.

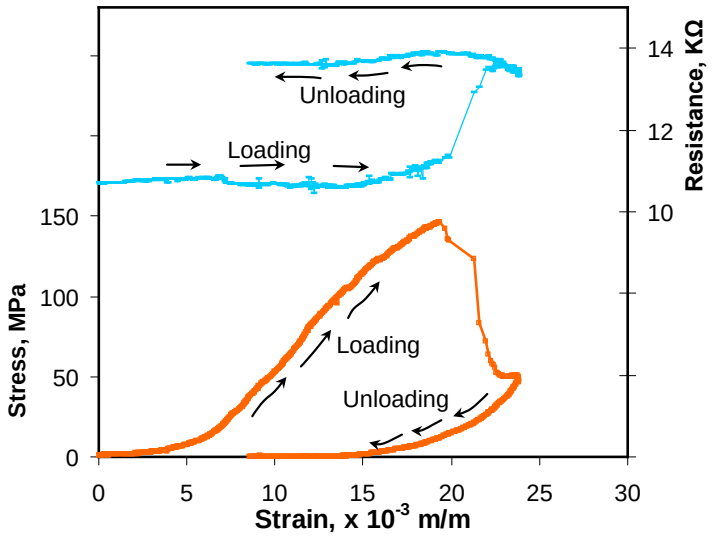

Figure 22. Stress versus strain and DC electrical resistance measured during a compression test of an indented GFRP tube made with 1 wt% CNF/epoxy.

4.4. Damage Detection in Glass/Epoxy Composites using DC Electrical Resistance Measurement Method and Advanced Electrode Configuration

Carbon black (CB) was selected as the nanofiller for the GFRP laminates used in this segment of the investigation because of it better potential for anisotropic conductivity tailoring, according the results presented earlier in this report. In addition, a novel arrangement of electrodes consisting of parallel or crossed arrangements of carbon tows was employed in order to allow the in-plane location of damage in the laminate to be determined.

CB-filled glass/epoxy composite plates with a $[0/90]_{13s}$ lamination arrangement were produced using hand lay-up, vacuum bag consolidation and cure (Figure 23). The plates had 150×150× 4 mm dimensions. The dimensions of the plates were chosen such that the plates can be quasi-statically indented according to ASTM D6264 (2007). To enable localizing of the damage using the DC electrical resistance method, electrodes consisting of 10 pieces of Hexcel AS4-12K carbon fiber tow were placed on top and bottom of the impregnated layers, with five tows placed on top and the other five placed on bottom. This type of co-cured electrode can be expected to be compatible with GFRP laminates in terms of strain capacity and adhesion.

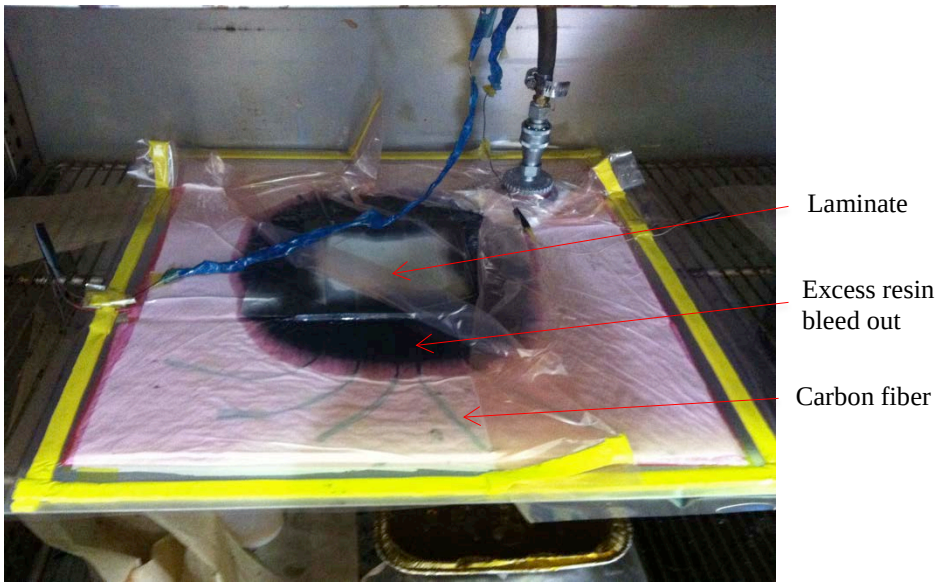

Figure 23. Vacuum bagging of a CB-filled glass/epoxy plate before curing.

Aluminum foils were present on the top and bottom surfaces of the plates for alignment purposes. Alignment was done at 1000 V/cm AC field strength and 1 kHz frequency. Once a plate was cured, it was taken out of the mold and the resistance measurements were done using aluminum foil and different combinations of carbon tows after peeling off the aluminum electrodes. For the measurements from aluminum, copper wires were attached to aluminum using copper tape that has conductive adhesive. For the measurements conducted by using carbon tows as electrodes, measurement probes were directly connected to the tows (Figure 24). DC resistance measurements were done with a digital multimeter. Based on the cured laminate thickness and the known amount of glass

fiber in the laminates, the fiber volume fraction of the plates was calculated to be approximately 59%.

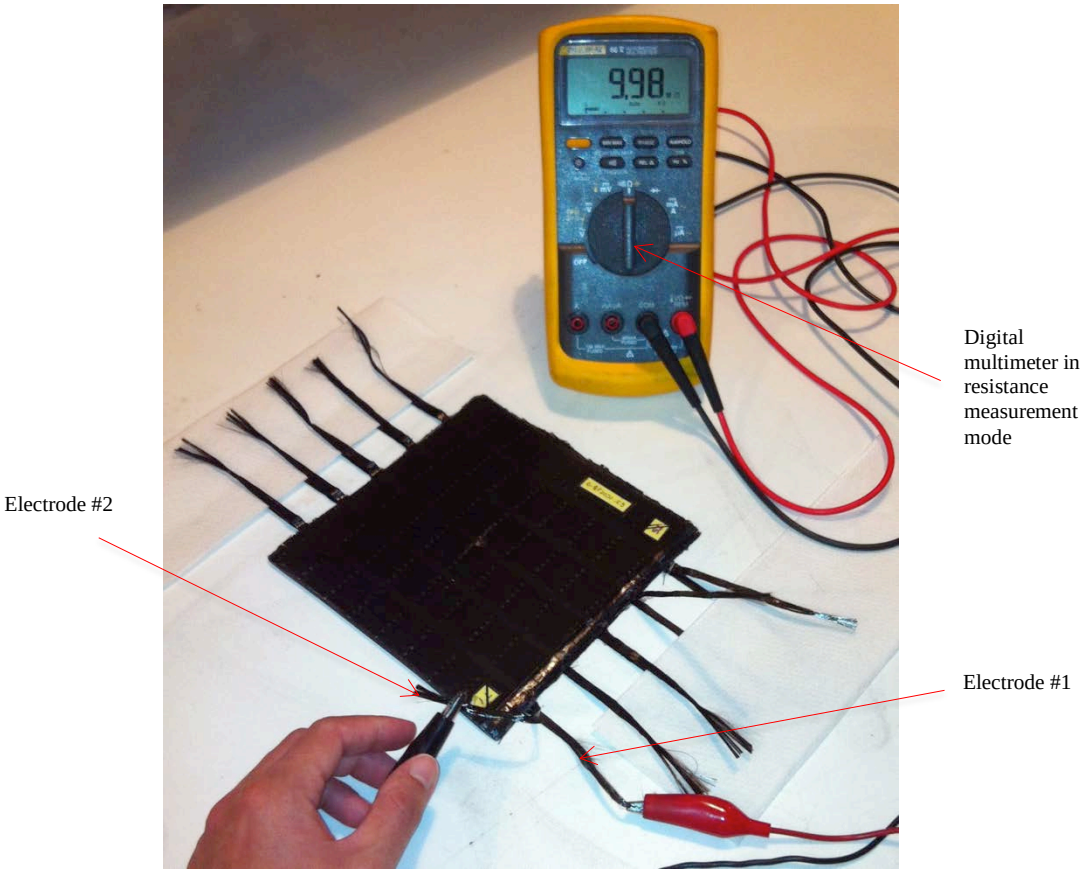

Figure 24. Resistance measurements of CB-filled glass/epoxy composite using carbon tows.

In order to introduce damage to the composite plates, indentation tests were conducted according to ASTM D6264 (2007) standard (Figure 25). Edge-supported configuration of the standard was used during the tests using an aluminum plate that has 203×203×25.4 mm dimensions and a 127-mm-diameter hole centered in the middle. The hemi-spherical tip of the indenter was positioned at the center of the composite plates, and the tests were conducted with a crosshead displacement rate of 1.25 mm/min. The displacement of the crosshead was measured by using a laser extensometer. Plates were indented until 4500 N and resistance measurements were conducted.

Ultrasonic C-scans were performed on the plates to detect the place of the damage inside the composites (Figure 26). The plate to be tested was immersed in water and was tested in through transmission mode. A pair of 2 MHz, 0.75 inch diameter planar transducers was used during the tests. After 4500 N loading, C-scans were conducted to determine the place and the size of the damage introduced during the indentation tests. After c-scan measurements, plates were dried at 100°C for 7-10 hours to eliminate the water residues on the plates due to immersing in water during C-scan and were placed in desiccators after drying.

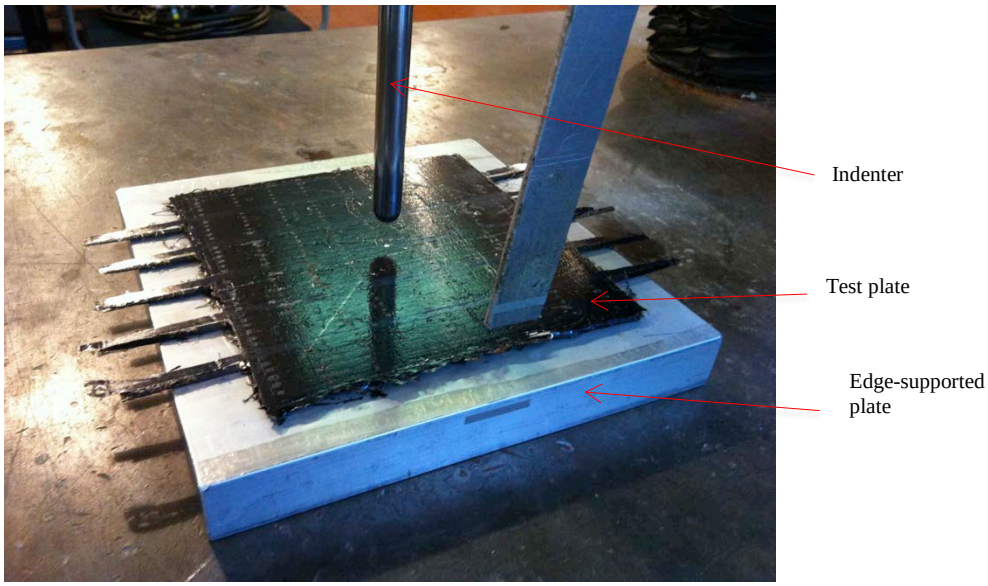

Figure 25. Indentation test setup for flat plates.

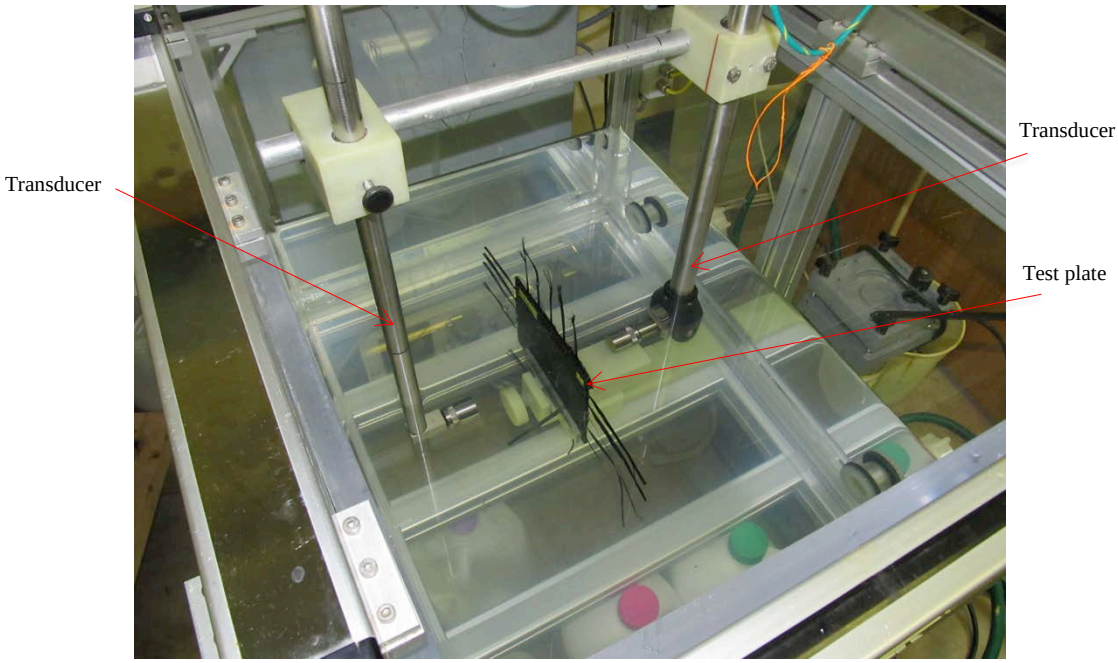

Figure 26. Ultrasonic C-scan test in through transmission mode for a perpendicular electrode configuration CB-filled glass/epoxy plate.

The configuration of the CB/glass/epoxy plates produced for damage detection tests are given in Table 1. In these plates, the effect of thickness, CB alignment and electrode configuration were examined. Two different electrode configurations were tested: parallel and perpendicular. In parallel electrode configuration, carbon fibers on the top and bottom surfaces are parallel to each other, going in the same direction, whereas in the

perpendicular electrode configuration these electrodes lie in directions that are perpendicular to each other. Schematic illustrations of these configurations are given in Figure 27. Each carbon fiber was numbered and this numbering was used for the electrical resistance measurements. In all of the plates, same CB concentration was used. One plate was made without any electric field to see the effect of CB alignment, and one plate was produced to be thicker than the others to see the effect of thickness on the damage detection capability.

Table 1. Configuration of CB/glass/epoxy plates produced for damage detection tests.

Name	Thickness (mm)	CB wt%	Electric Field for CB alignment	Electrode Material	Electrode Configuration
P1	4	0.5	1000 V/cm & 1 kHz	Carbon Fiber	Parallel
P2	4.5	0.5	1000 V/cm & 1 kHz	Carbon Fiber	Parallel
P3	4	0.5	1000 V/cm & 1 kHz	Carbon Fiber	Perpendicular
P4	4	0.5	-	Carbon Fiber	Parallel

After curing and demolding, DC resistances of the plates through the thickness were measured by using the aluminum foil electrodes that are on the top and bottom surfaces. By using the measured resistances and the geometry of the plate, through-thickness DC electrical conductivity for each plate was calculated, as given in Table 2. Carbon fibers were not used for calculating the DC conductivity, since the effective cross-sectional area between fibers is not exactly known.

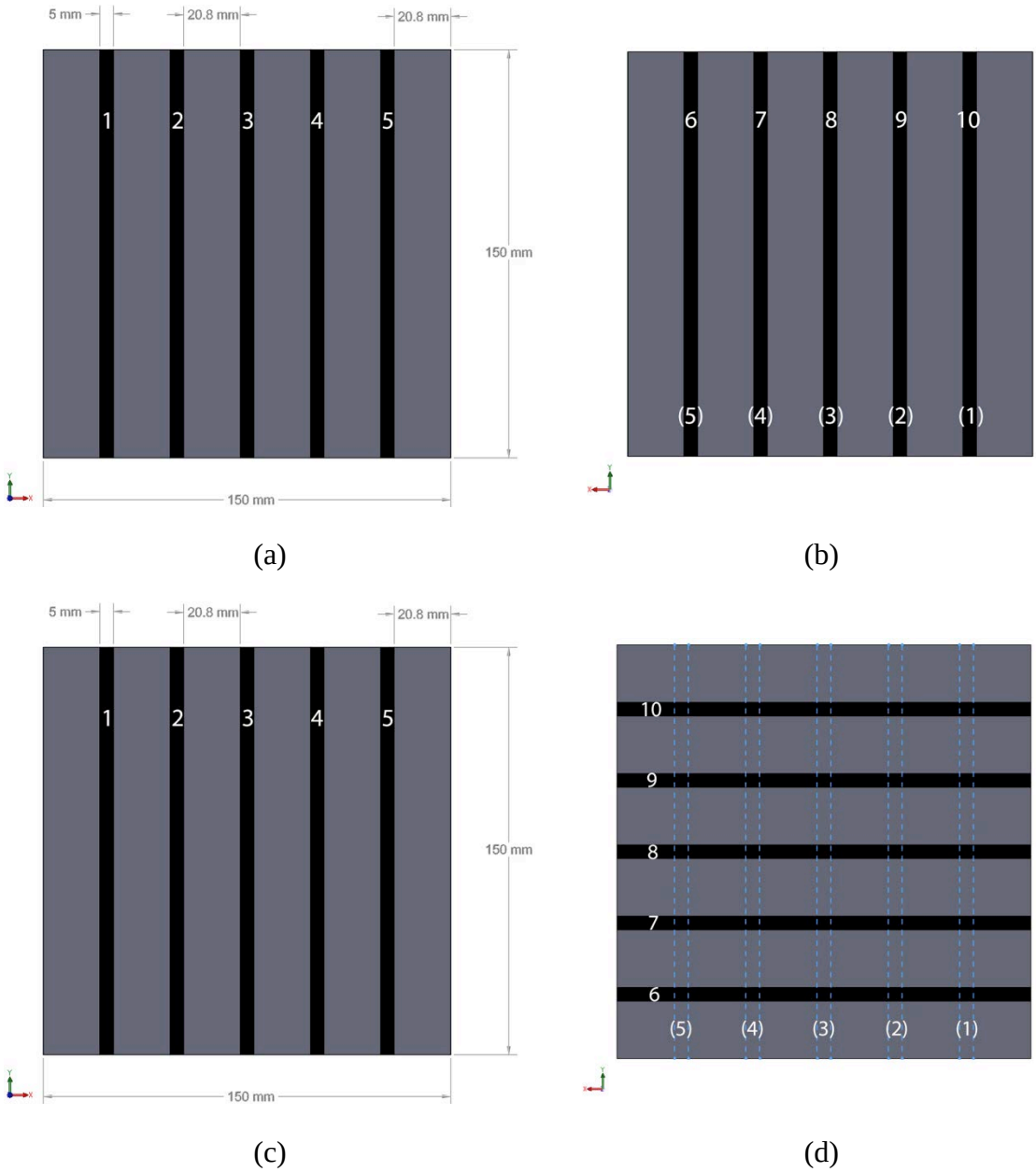

Figure 27. Parallel electrode configuration (a) top view, (b) bottom view. Perpendicular electrode configuration (c) top view, (d) bottom view. Black stripes represent the carbon fibers, and each fiber is denoted by a number.

Table 2. Through-thickness DC resistance and conductivity of the test plates.

Name	DC Resistance (MΩ)	DC Conductivity (S/m)
P1	0.726	2.45×10^{-7}
P2	2	1.04×10^{-7}
P3	0.853	2.08×10^{-7}
P4	200	9.01×10^{-10}

Following the determination of the conductivity of each plate, aluminum foils were peeled off the surfaces to eliminate the conductive path between carbon fibers. The resistance measurements conducted by using carbon fibers with the presence of aluminum electrodes resulted in the same resistance readings for each carbon fiber pair. This is due to the conductive aluminum covering the entire surface and acting as a one-piece electrode connecting each carbon fiber. Therefore, in order to eliminate this effect, aluminum foils were peeled off after measuring the overall conductivity of the test plates and resistances of different regions of the plates were measured.

After the indentation tests, resistance of test plates P1, P2, P3 and P4 were re-measured to see the change in resistance due to loading. In order to prove the existence of damage in each plate, and to find its location, ultrasonic C-scan tests were conducted after 4500 N indentation tests. Results of resistance change measurements and C-scans are given in Figure 28. For parallel electrode configuration plates (P1, P2 and P4), it was only possible to detect the location of damage along one direction. For P1 and P2, the location of damage along the horizontal axis predicted from electrical resistance measurements matches well with the c-scan results. As seen, it is possible to detect damage in specimens that have different thicknesses. For P4, which has random CB, the resistance measurements showed the damage to be towards the right of the specimen, in a region between 4^{th} and 7^{th} electrodes. However, when its C-scan was investigated, damage was detected to be towards the middle of the plate. Moreover, there exists a wide region at which resistance change is negative, which is not an expected result. As seen, for the same CB concentration and plate configuration, CB alignment results in higher sensitivity for damage detection in glass/epoxy plates. For plate P3, it was possible to locate the damage horizontally as well as vertically. This is due to the presence of electrodes that lie in perpendicular directions. When the electrical resistance measurements were compared with the C-scan result, it is further seen that the two methods coincides well.

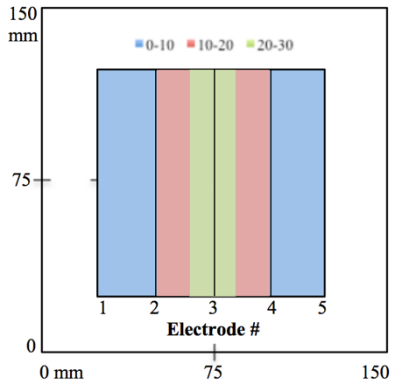
150
mm
0-10
10-20
20-30
75
0
1
2
3
4
5
Electrode #
0 mm
75
150

(a)

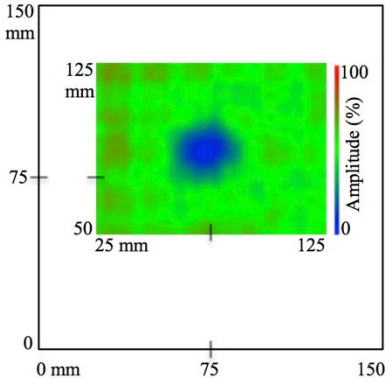
150
mm
125
mm
100
Amplitude (%)
75
50
0
25 mm
125
0 mm
75
150

(b)

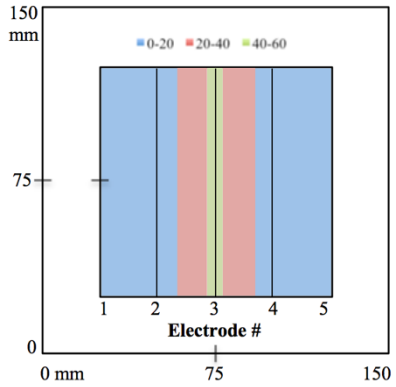
150
mm
0-20
20-40
40-60
75
0
1
2
3
4
5
Electrode #
0 mm
75
150

(c)

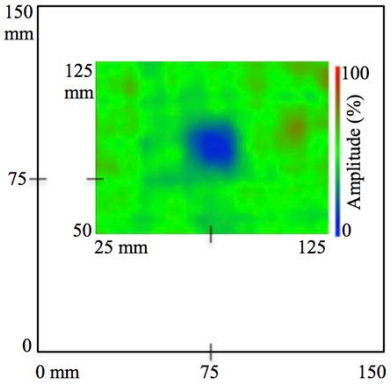
150
mm
125
mm
100
Amplitude (%)
75
50
0
25 mm
125
0 mm
75
150

(d)

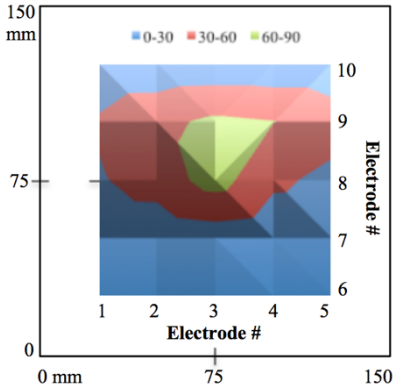
150
mm
0-30
30-60
60-90
10
9
8
7
6
Electrode #
75
0
1
2
3
4
5
Electrode #
0 mm
75
150

(e)

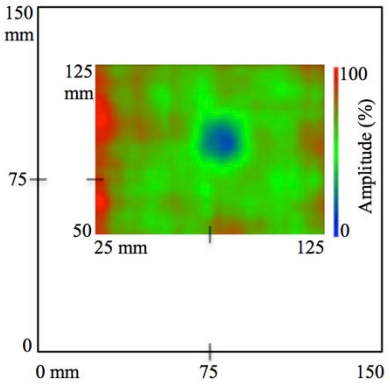
150
mm
125
mm
100
Amplitude (%)
75
50
0
25 mm
125
0 mm
75
150

(f)

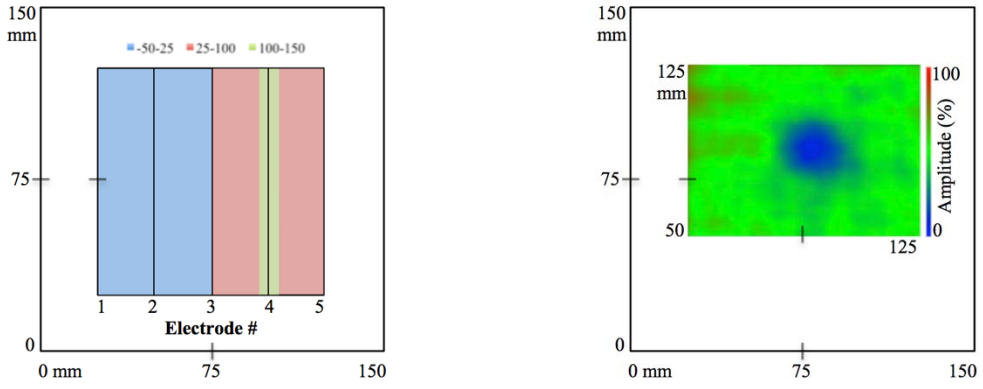

(g) (h)

Figure 28. Plots of percent resistance change in experimental test plates (a) P1, (c) P2, (e) P3, and (g) P4 after 4500 N indentation loading and corresponding C-scans for (b) P1, (d) P2, (f) P3, and (h) P4.

Based on the results observed in this investigation, it is understood that preferential alignment of CB through the thickness enhances the sensitivity to damage detection by forming continuous conductive chains that break due to the damage formation. In addition to providing a better sensitivity, alignment also enables the use of less complicated instrumentation for resistance measurement due to increased conductivity through the thickness.

The experiments conducted with using parallel and perpendicular electrode configurations, which are proposed in this investigation, show that it is possible to detect the location of damage by using continuous carbon fiber electrodes on top and bottom surfaces of the composites. Until now, grid-like electrodes on a surface of a composite, or conductive paints on different surfaces of test coupons were employed to detect different types of damage (Nofar et al., 2009; Gao et al., 2011; Zhang et al., 2012; Hoa and Naghashpour, 2013; Viets et al., 2013). In this investigation, continuous strip-like electrodes were proposed in different configurations that enabled utilizing a simple measurement technique. Between the two new electrode configurations, the perpendicular configuration was observed to be more advantageous than the parallel configuration due to the presence of electrodes in perpendicular directions, which allow the detection of damage in two dimensions. Moreover, it is also shown that carbon fibers can be effectively used as measurement electrodes. This may especially be beneficial in industrial applications, due to the good bonding of carbon fibers with the main composite structure.

4.5. Tomographic Conductivity Imaging for Structural Health Monitoring and Damage Detection

Identifying conductivity changes in nanofiller-rich matrices is a promising area of structural health monitoring. Conductivity depends on the formation of well-connected networks of nanofillers, and matrix damage severs the connection between fillers thereby greatly reducing conductivity. Identifying conductivity changes can therefore be used to track damage. In the following, state-of-the-art in tomographic conductivity-based health

monitoring is tersely summarized. Next, the theoretical background of tomographic conductivity imaging is explained. Damage detection is demonstrated on two materials – a glass fiber/epoxy with CB filler and a CNF/epoxy. These results indicate that tomographic conductivity imaging is viable for SHM. Next, methods of enhancing damage detection by leveraging the unique properties of nanocomposites are discussed. It has been found that exploiting conductivity evolution to eliminate baseline measurements is feasible. Analytical results also that piezoresistivity coupling enhances damage detection. And, lastly, it has been demonstrated that nanofiller alignment improves sensitivity to damage.

Electrical impedance tomography (EIT) can spatially resolve conductivity changes, is minimally invasive, and can be employed in real time. These features make it an appealing SHM approach. EIT has received excellent treatment in tracking damage to CNT thin films (Hou, Loh, and Lynch, 2007; Loh et al., 2009) and cementitious structures (Hou and Lynch, 2009). Loyola et al. demonstrated the ability of EIT to detect damage to a GFRP manufactured with a CNT thin film sensing layer (Loyola et al., 2013). These works establish EIT as a viable health monitoring technique for nanofiller-rich matrices but have important limitations. Damage sufficiently removed from the sensing layer or sensing coat such as internal damage initiated by cyclic loading may go undetected. Superficial damage to the coating induced by hail, sleet, or dust in aerospace applications may also register as damage when there is no real threat to the structure. Lastly, the additional weight of a coating may be unpalatable for the design of weight-conscious aerospace structures. Nanofiller-rich epoxy matrices circumvent these limitations. Because the matrix permeates every layer, the composite is sensitive to both internal and external damage while retaining immunity to superficial damage. Nanofillers are also of negligible parasitic weight.

EIT minimizes the difference between experimental measurements and an analytical model in order to reproduce a domain's conductivity distribution. The difference is minimized by iteratively updating an initial conductivity estimate by a conductivity difference vector recovered from equation (1):

$$\boldsymbol{J}\Delta\boldsymbol{\sigma} = \boldsymbol{V}_e. \tag{1}$$

Here, $\boldsymbol{J}$ is known as the sensitivity matrix and must be inverted. However, it is severely rank deficient, and Tikhonov regularization is required to recover $\Delta\boldsymbol{\sigma}$ as shown in equation (2),

$$\Delta\boldsymbol{\sigma} = (\boldsymbol{J}^T\boldsymbol{J} + \alpha^2\boldsymbol{L}^T\boldsymbol{L})^{-1}\boldsymbol{J}^T\boldsymbol{V}_e. \tag{2}$$

$\boldsymbol{L}^T\boldsymbol{L}$ is the regularization term, and its contribution is controlled by α^2. Herein, the discrete Laplace operator is employed as regularization.

4.5.1. EIT on Glass Fiber/Epoxy with Chained Carbon Black

The ability of EIT to capture damage to glass fiber/epoxy laminates with CB chained through the plate thickness has been demonstrated. There were three goals to this study:

(1) determine the sensitivity of EIT to through-hole damage on glass fiber/epoxy with aligned CB filler; (2) demonstrate the ability of EIT to capture multiple damages; and (3) demonstrate the ability of EIT to capture impact damage.

Sensitivity to damage is an important aspect of health monitoring and damage detection. Therefore, increasing levels of through-hole damage were induced in order to determine the sensitivity of EIT on glass fiber/epoxy with aligned CB. More specifically, a 1.5875 mm diameter hole was drilled through the specimen. The hole was subsequently bored out to diameters of 3.175 mm, 4.7625 mm, and 6.35 mm. EIT was performed after each new damage diameter. Figure 29 shows the results of this analysis.

To demonstrate the capability of EIT to detect multiple damages, a second hole was drilled through the glass fiber/epoxy plate. The second hole was initially 1.5875 mm in diameter. It was then bored out to 3.175 mm, 4.7625 mm, and 6.35 mm in diameter. EIT was performed after each new diameter. After the second hole was bored out to 6.35 mm, a third hole with a diameter of 6.35 mm was drilled. Figure 29 also shows the results of these experiments.

Each image shown in Figure 29 is normalized by the same value – the maximum of the entire set of images. Normalizing the results in this manner enables them to be plotted on the same scale, and the influence of increasing damage on EIT reconstruction becomes obvious. However, this also causes the small through holes to appear much less prominently. Figure 30 shows the EIT images for a single 1.5875 mm hole and a single 3.175 mm hole each plotted individually. The 3.175 mm hole is immediately visible, but the 1.5875 mm hole is not as discernable from the image noise. It is therefore concluded that the lower limit of hole detection for glass fiber/epoxy with CB via EIT is between 1.5875 mm and 3.175 mm.

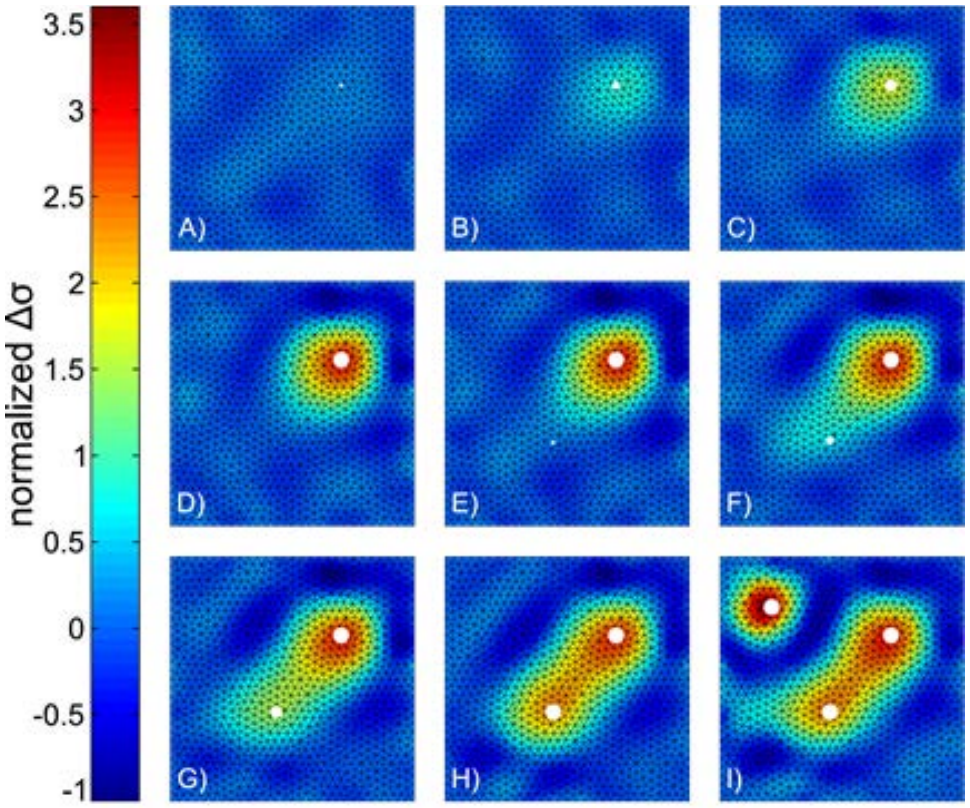

Figure 29. Sensitivity and multiple damage detection. Each image is normalized by the same value – the maximum of the entire set of images. The undamaged baseline is subtracted. Through hole size and location indicated by white circles. Diameters of each through hole are as follows. A) 1.59 mm. B) 3.18 mm. C) 4.76 mm. D) 6.35 mm. E) 6.35 mm and 1.59 mm. F) 6.35 mm and 3.18 mm. G) 6.35 mm and 4.76 mm. H) 6.35 mm and 6.35 mm. I) 6.35 mm, 6.35 mm, and 6.35 mm.

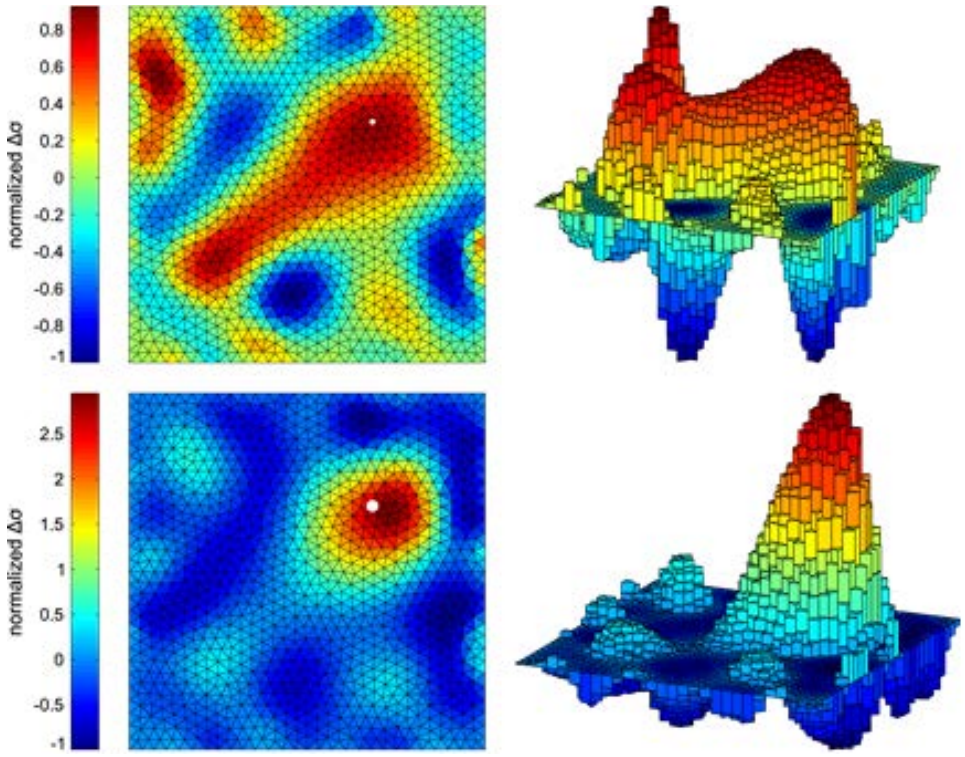

Figure 30. Sensitivity to small through holes. Images are each individually normalized by their respective maximum values. The undamaged baseline is subtracted. Through hole size and location indicated by white circles. Top: EIT reconstruction with a single 1.59 mm diameter hole. Bottom: EIT reconstruction with a single 3.18 mm diameter hole.

Drop tower impacts were performed on the second glass fiber/epoxy plate. The plate was cut to approximately 101.6 mm × 152.4 mm in order to accommodate the impact machine with simply-supported, symmetric boundary conditions. An impact of 50 Joules was performed. This impact resulted in a slight indentation at the impact location and the formation of a crack initiating at the indentation and running along the fiber direction as shown Figure 31, and the EIT reconstruction is shown in Figure 32. These results demonstrate that EIT is a viable and accurate method of detecting impact damages to glass fiber/epoxy laminates with conductive matrices.

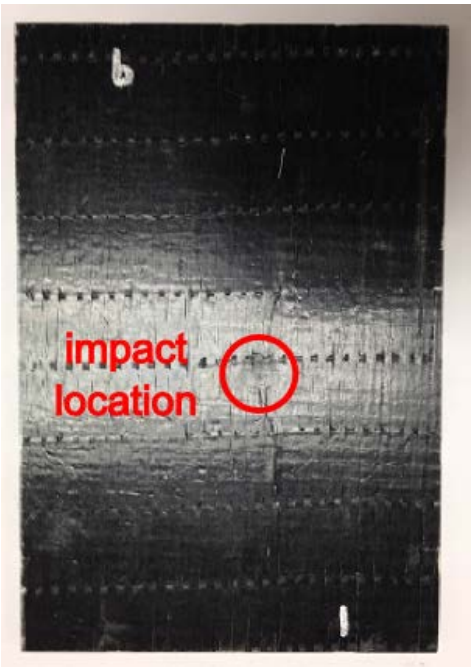

Figure 31. Impacted glass fiber/epoxy laminate plate.

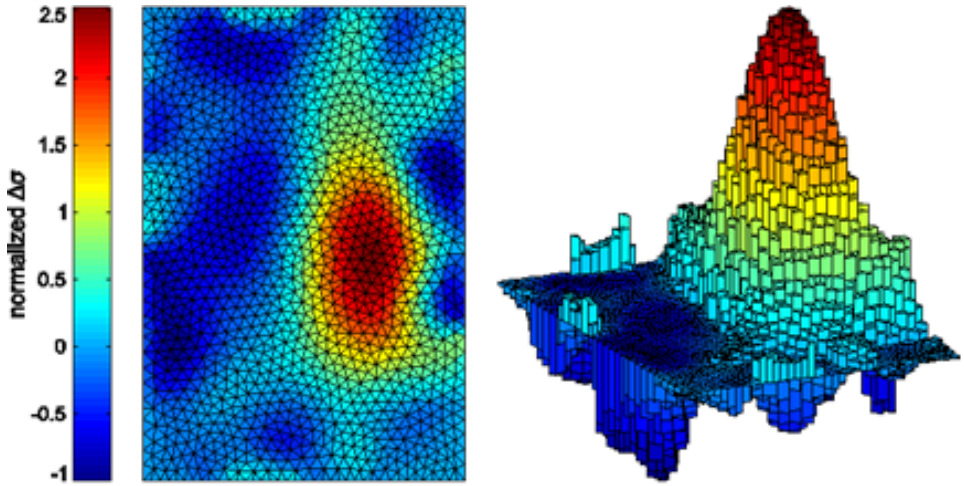

Figure 32. EIT image of impact-damaged glass fiber/epoxy laminate plate with aligned CB filler. EIT accurately locates the impact location and even produces a ridge-like artifact which coincides with the location of the crack damage shown in Figure 31.

4.5.2. Conductivity Evolution and Damage Detection in Carbon Nanofiber/Epoxy via EIT

Nanocomposite conductivity is dependent upon well-connected networks of nanofillers. Fillers are not in direct physical contact but separated by a thin layer of matrix material. Electrons are able to tunnel through this matrix layer and between sufficiently proximate fillers thereby enabling composite conductivity. Mechanically straining a nanocomposite will alter the spacing between fillers. The resistance between fillers depends exponentially on their separation meaning even slight strains can greatly influence conductivity (Hu et al., 2010; Hu et al., 2008; Simmons, 1963). Temperature increases due to electrical loading will cause thermal expansion in the matrix thus causing fillers to drift apart. This will result in decreased composite conductivity as observed by Kumar et al. (2007) and Mei et al. (2008). A method of imaging conductivity evolution due to electrical loading has been developed in order to explore evolution imaging as a method of eliminating the need for an undamaged-baseline EIT image to detect damage. In other words, electrode placement errors manifest as conductivity errors in EIT that may be falsely identified as damage. Consequently, damage is detected by taking the difference between an undamaged EIT image and a damaged EIT image. EIT was performed on a CNF/epoxy plate. Damage was induced by drilling a 6.35 mm diameter through-hole. Figure 33 shows the errors in the resulting EIT image, and Figure 34 shows how damage is recovered by taking the difference between the damaged and undamaged images.

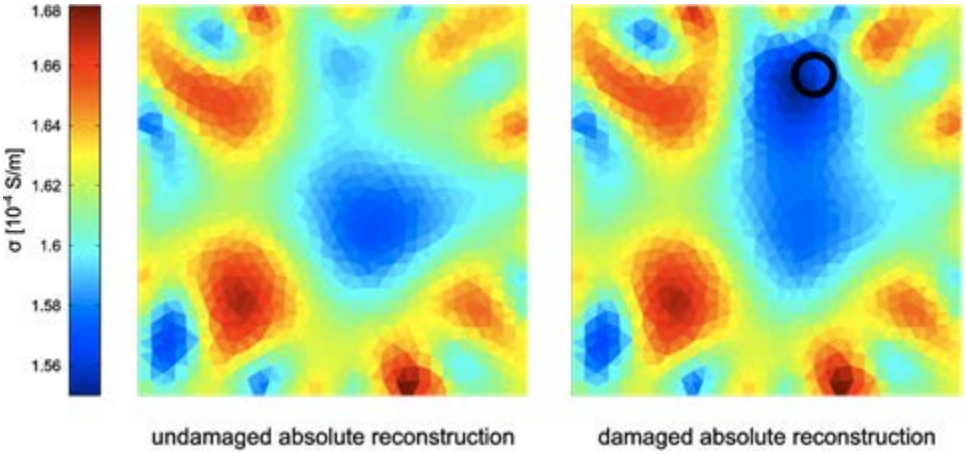

Figure 33. Undamaged and damaged EIT reconstructions of a CNF/epoxy plate. Note the prevalence of conductivity artifacts that may be falsely identified as damage. True damage size and location is indicated by the black circle.

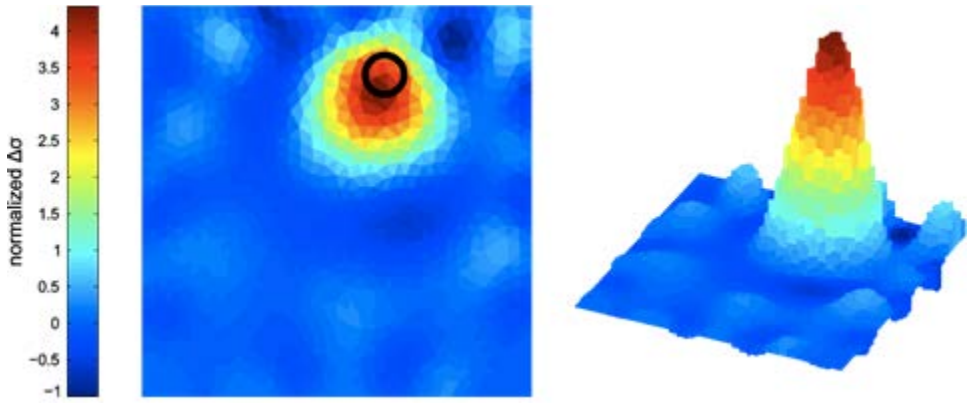

Figure 34. Damage is accurately located by taking the difference between the damaged and undamaged images shown in Figure 33. True damage size and location is indicated by the black circle.

Based on measurement observations and existing literature (Loh et al., 2009), the conductivity of the *e*th element in the EIT reconstruction is proposed to evolve as:

$$\sigma_e(t) = (\sigma_i - \sigma_f)e^{-\beta t} + \sigma_f + \varepsilon \tag{3}$$

Here, σ_i is the initial conductivity, σ_f is the steady state conductivity, ε is an error term which is the result of electrode misplacements, and the exponent is a function of current magnitude. Differentiating equation (1) with respect to time will eliminate the error term as shown in equation (4),

$$\boldsymbol{J}\frac{\partial \boldsymbol{\sigma}}{\partial t} = \frac{\partial \boldsymbol{V}_m}{\partial t}. \tag{4}$$

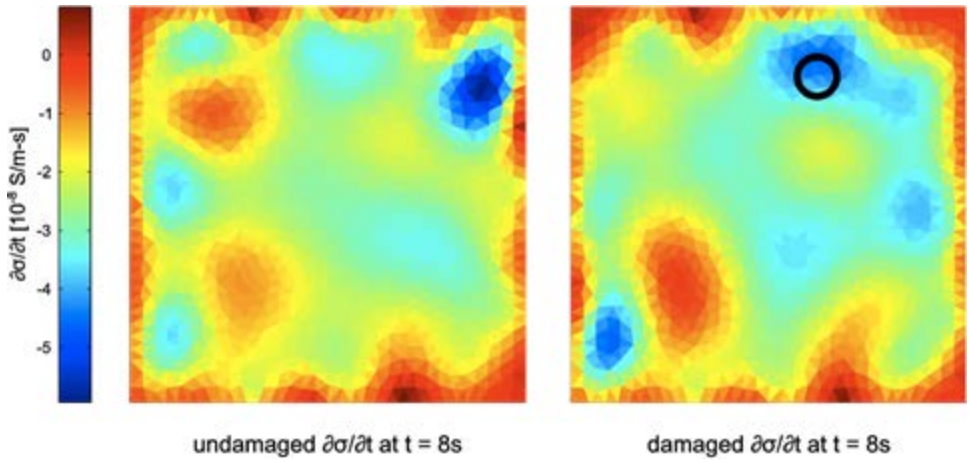

Figure 35. Undamaged and damaged conductivity rate images at t = 8 s. True damage size and location is indicated by the black circle.

As shown to the right in Figure 35, there is a region coinciding with the damage region where the conductivity is rapidly decreasing. The rate of change of the EIT reconstruction for the damaged region should be rapidly decreasing because the reconstruction process

is trying to reproduce a region of no conductivity. However, that this is due to damage is not definitive due to regions of rapid conductivity evolution in the lower left corner. It is speculated that the CNF distribution influences the rate of conductivity change. In regions of low filler concentration, the material is more sensitive to thermal expansion because there are fewer nanofiller junctions and the loss of even a few tunneling paths due to expansion will have a large influence to reduce conductivity. Conversely, regions of higher filler concentration can afford to lose more tunneling paths and remain conductive. Therefore, the conductivity evolves less rapidly. Other researchers have observed a similar increase in sensitivity to strain for nanocomposites with lower weight fractions (Hu et al., 2010; Hu et al., 2008; Kang et al., 2006). The initial results in Figure 35 are encouraging but not as conclusive as Figure 34. Nonetheless, because reconstruction errors in Figure 33 have been largely eliminated, this approach merits further investigation.

4.5.3. EIT Enhancement through Piezoresistive Coupling

Mechanically straining a nanocomposite will alter the spacing between fillers thereby changing the conductivity of the composite. This property can be leveraged to enhance EIT. Recall also that the EIT sensitivity matrix $\boldsymbol{J}$ is rank-deficient. It has been demonstrated that the rank of $\boldsymbol{J}$ can be enhanced by supplementing equation (1) with additional measurements taken as the composite is strained. Let the strained and unstrained conductivities be related as,

$$\hat{\boldsymbol{\sigma}} = \boldsymbol{G}\boldsymbol{\sigma}. \tag{5}$$

By performing EIT on both the strained and arbitrarily many unstrained states, equation (1) can be rewritten in light of equation (5) as,

$$\begin{bmatrix} \boldsymbol{J} \\ \vdots \\ \hat{\boldsymbol{J}}^n \boldsymbol{G}^n \end{bmatrix} \boldsymbol{\Delta\sigma} = \begin{bmatrix} \boldsymbol{V}_e \\ \vdots \\ \hat{\boldsymbol{V}}_e^n \end{bmatrix}. \tag{6}$$

The augmented sensitivity matrix can be inverted and the conductivity change vector recovered by again employing Tikhonov regularization. Analytical studies were conducted to assess the validity of this approach. The analytical studies used a reference finite element mesh with simulated damage that EIT must reproduce. The rank of the augmented sensitivity matrix was calculated by singular value decomposition (SVD) and compared to the rank of the unenhanced sensitivity matrix as shown in Figure 36. The enhancement of the rank of the sensitivity matrix was found to be proportional to the number of enhancing strain fields used.

Figure 37 shows the results of enhancing EIT through simulated strain coupling. This shows that it is possible to either increase the resolution of EIT for a fixed number of electrodes or to detect damage using considerably fewer electrodes.

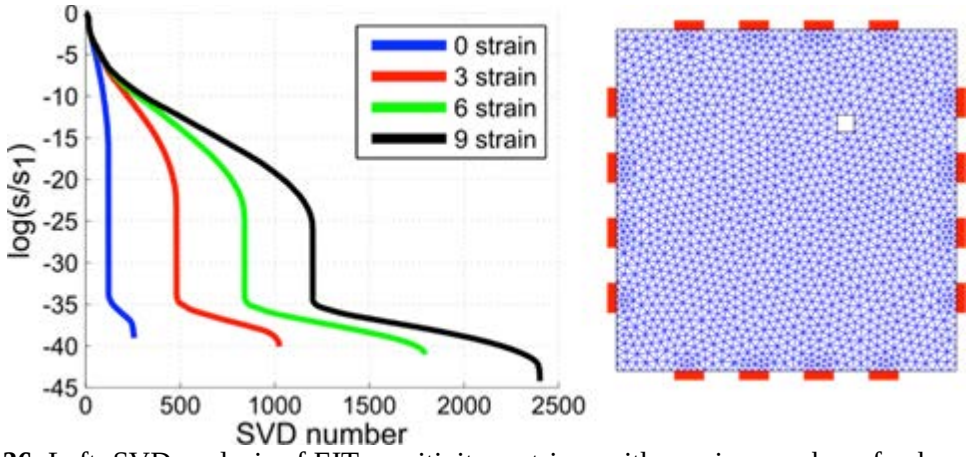

Figure 36. Left: SVD analysis of EIT sensitivity matrices with varying number of enhancements. Right: reference finite element mesh with simulated damage.

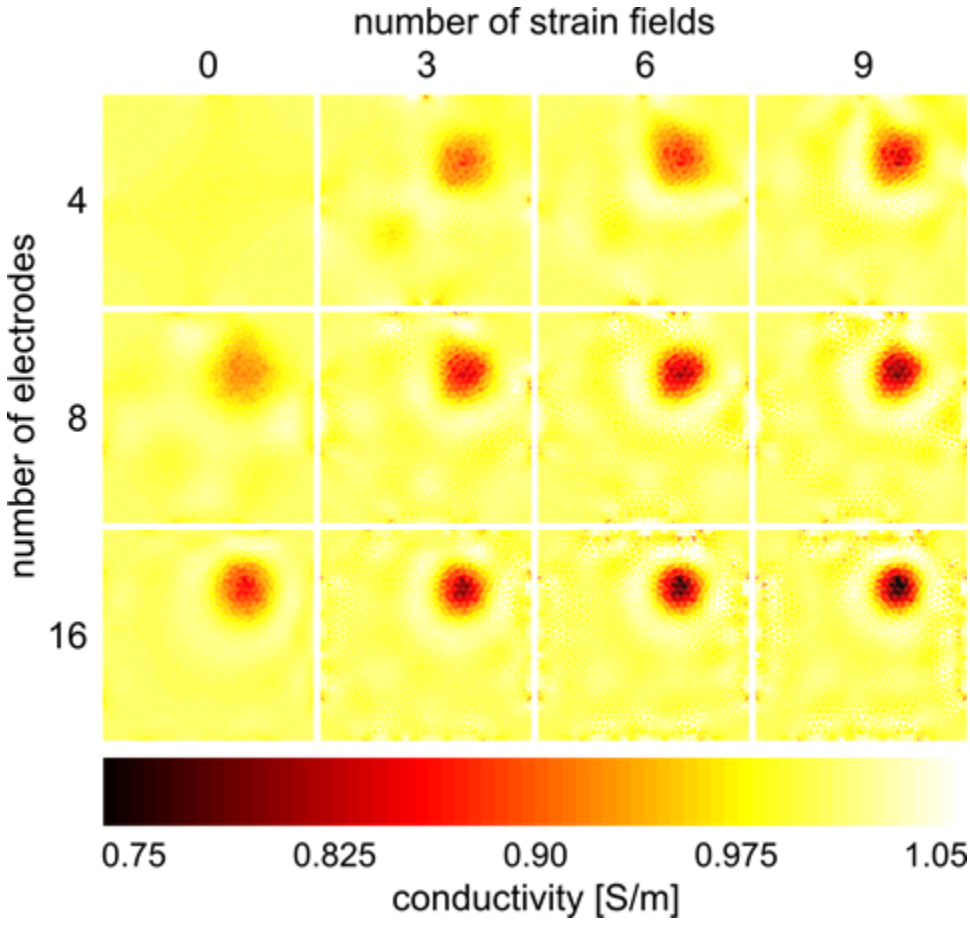

Figure 37. Enhanced EIT images of simulated damage with artificial strain coupling.

Having demonstrated the enhancement afforded by strain coupling, a piezoresistive model was developed. A variety of piezoresistivity models exist for nanocomposites (Hu et al., 2008; Hu et al., 2010), but because these models track individual fillers, they are computationally unpalatable for structural-scale analysis. Therefore, an analytical model

was developed CNT composite piezoresistivity which accounts for the influence of strain on volume fraction, critical volume fraction, percolation probability, and inter-filler spacing. The model predictions agree well with experimental results in existing literature, and it has the ability to analyze the piezoresistive response of CNT composites under arbitrary straining thereby making it adaptable to finite element formulation. Figure 38 shows a comparison of the model predictions with experimental results in existing literature.

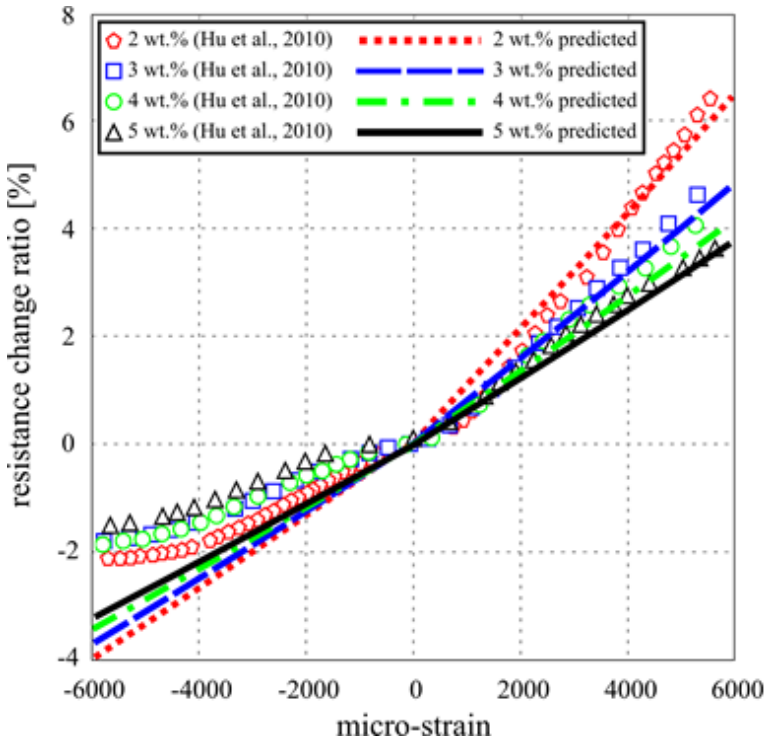

Figure 38. Comparison of predicted resistance changes to experimental results in literature for a CNT composite.

4.5.4. Enhanced Damage Sensitivity through Carbon Nanotube Alignment

Enhancing the sensitivity of nanocomposites to delamination through CNT alignment was investigated. Monte Carlo simulations were used to model both random and aligned planar CNT distributions from which it was found that alignment results in considerable conductivity enhancement in the alignment direction. Conversely, significant conductivity was lost perpendicular to the alignment direction. Random CNT distributions were found to be electrically isotropic.

To investigate the effect of the CNT alignment on damage sensitivity, finite element models of 1 cm × 1 cm squares with the conductive properties of aligned and random CNT networks were developed. Damage is simulated as a 1 mm × 0.1 mm open cut and rotated through several angles as shown in Figure 39. Sensitivity to damage was defined as the percent change in conductivity between an undamaged and a damaged specimen.

These results have shown that highly aligned nanofiller networks are very sensitive to damage perpendicular to the alignment direction.

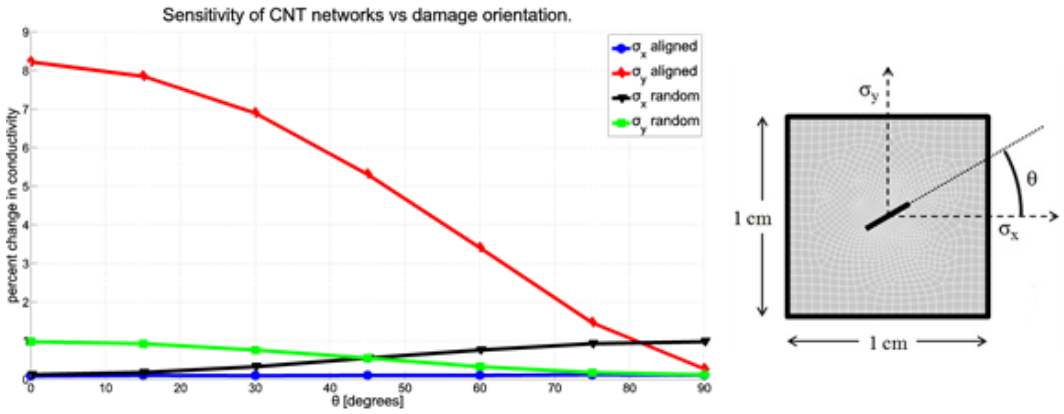

Figure 39. Left: percent change in conductivity due to damage versus damage orientation. Right: damage geometry with the damaged area enlarged for clarity.

Finally, EIT was used to detect simulated damage to two cross-sections – one with aligned CNT conductive properties and the other with random CNT properties. In order to do this, an anisotropic EIT routine had to be developed. Consider the *i*th update iteration of the *k*th element:

$$\boldsymbol{\sigma}_{\boldsymbol{i+1}}^{\boldsymbol{k}} = \boldsymbol{\sigma}_{\boldsymbol{i}}^{\boldsymbol{k}} + \boldsymbol{\delta\beta\sigma}_{\boldsymbol{i}}^{\boldsymbol{k}}. \tag{7}$$

The scalar conductivity coefficient in equation (1) is now replaced by a symmetric matrix for each element, and equation (7) seeks to find a coefficient by which the conductivity matrix is updated. Figure 40 shows the result of using EIT to detect a small crack to a material with random CNT properties (isotropic conductivity) and a material with highly aligned CNT properties (anisotropic conductivity). This demonstrates that alignment greatly enhances sensitivity to damage which occurs perpendicular to the alignment direction. Therefore, aligning fillers through a composite plate will enhance sensitivity to delamination.

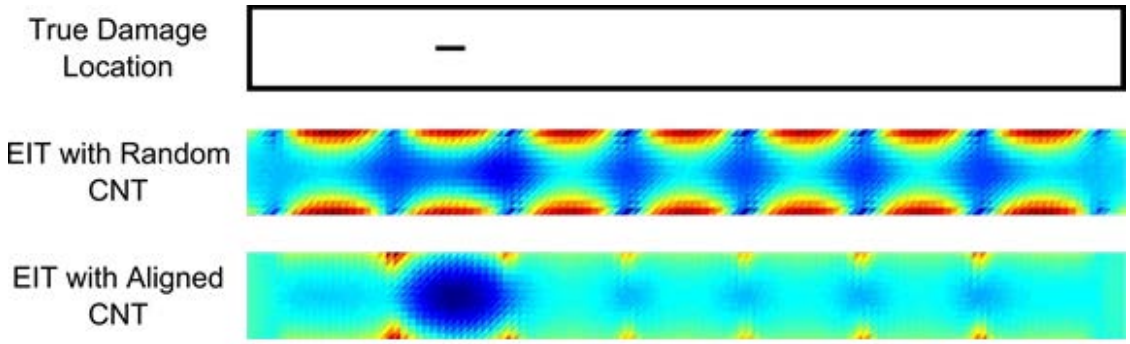

Figure 40. Enhanced detectability of damage with CNT alignment and EIT.

5. Summary

Short conductive nanofillers such as CB and short CNTs have been shown to be superior to high-aspect ratio nano-fillers such as long CNFs or CNFs for tailoring the electrical conductivity of epoxy and glass reinforced epoxy composites. Anisotropic electrical networking is favored by smaller particles that can be easily manipulated by dielectrophoretic forces provided by the AC electric field. Parametric investigations have shown that conductivity through the thickness direction of GFRP laminates can be increased by a factor of 10^4 by using relatively small amounts of CB and properly selected filler concentration and AC electric field prior to cure. This result is three orders of magnitude better than the previous state-of-the-art in electrical conductivity tailored GFRP. The maximum ratios of through-thickness to in-plane conductivities obtained in unidirectionally reinforced GFRP were roughly 3.3 for σ_3/σ_2 and 1.6 for σ_3/σ_2. This is the first time, to the authors' knowledge, that such an increase in through-thickness conductivity, anisotropy ratio greater than 1, and same order of magnitude conductivities in all three principal directions of UD glass/epoxy composites have been demonstrated, which should prove useful in future efforts to tailor the electrical properties of this type of material. Electrical tailoring was not highly sensitive to AC frequencies in the range of 100 to 10,000 Hz. Generally speaking, maximum electrical anisotropy was able to be obtained in materials with minimum electrical conductivity. Excessive conductivity prior to the application of electric field implied the existence of a percolated network of particles, which prevents the effective dielectrophoretic rearrangement of the particles that is necessary for tailoring the anisotropic conductivity.

Preliminary investigations of interlaminar crack growth detection using rudimentary full-surface electrodes on GFRP laminates with aligned CNT and CNF fillers were used to demonstrate the basic concept of monitoring crack growth using conductive fillers. Mode I and mode II crack growth in UD GFRP laminates as well as mixed mode growth of indentation damage in a multidirectionally reinforced GFRP cylindrical tube were demonstrated. To the knowledge of the authors, this is the first application of nanofiller alignment and ER-based damage evaluation to filament wound GFRP composites. It is a first step in the wider application of the ER method in generally-shaped structures.

CB-filled cross-ply GFRP composites with and without CB alignment and an advanced electrode configuration were used to demonstrate the ability of the ER method to determine the in-lane location of quasi-static indentation damage. The electrodes consisted on carbon fiber tows co-cured on the surface of the laminates. The location of the damage determined by the ER method with crossed carbon fiber electrodes compared exceedingly well with ultrasonic C-scan measurements only when CB alignment was applied. This result points the way to future development of full-area damage sensing with electrical connections only around the edges of the composite structure.

EIT has been investigated as a health monitoring technique for electrically conductive nanocomposites. It has been demonstrated that EIT can detect damage artifacts smaller than 3.175 mm in glass fiber/epoxy laminates with aligned CB filler. Impact damage has

also been accurately imaged in this material. EIT was also able to locate damage to a CNF/epoxy composite material.

Various methods of enhancing EIT for health monitoring have been investigated. Conductivity evolution imaging shows promise as a method to eliminate the need for an undamaged baseline. EIT resolution can be enhanced or the number of electrodes needed to perform EIT decreased by coupling EIT with piezoresistivity. To that end, a piezoresistivity model has also been developed to predict changes in conductivity as a function of strain. These predictions agree favorably with experimental results in existing literature, and the piezoresistivity model is amenable to finite element analysis. Lastly, analytical simulations have shown that sensitivity to damage and damage detectability are greatly enhanced through CNT alignment.

6. Technology Transfer

Dr. Dy Le (Army ARL- VTD, Aberdeen, MD) and Col. Reed Young (ARO) visited Penn State for a kickoff meeting in October 2010. Dr. James T. Ayers (Army ARL-VTD) visited Penn State to discuss our work and see our facilities in February 2011.

C. Bakis presented "Damage Detection in Glass/Epoxy Composites by Electrical Methods," to the annual meeting of the Ben Franklin Center of Excellence in Structural Health Monitoring, 4 August 2011, University Park, PA. Co-authors of this presentation were C. Bakis, K. W. Wang, Y. Zhu, F. Semperlotti, and T. Tallman.

Dr. Bakis is under contract with the Vertical Lift Consortium (AATD funding) to evaluate pre-commercial and commercial nano-filled carbon and glass fiber prepregs composites for the rotorcraft industry. The Technical Area of Joint Interest (TAJI) involves the Univ. of Texas at Arlington, Bell, Boeing, and Sikorsky. The main focus of this project is on mechanical performance, although a small part of the project concerns electrical property tailoring for lightweight lightning strike protection.

Dr. Bakis has been working on a Phase II Army SBIR with Nextgen Aeronautics on the use of nanoreinforcements in rocket motor casings for improved impact resistance. Among Army monitors in the bi-weekly telecons are Keith Roberts and Daniel Carter of the Aviation and Missile Research, Development, and Engineering Center (AMRDEC), Propulsion and Structures Directorate, Aerospace Materials, Redstone Arsenal, AL. Dr. Bakis' role in the project is to provide expertise to Nextgen on the use of nano-reinforcements in the rocket casing filament winding process to minimize the effect of blunt object impact on burst strength. The project was awarded a Phase II Extension for 2011-13.

Dr. Bakis wrote an ARL proposal to the 2014 Joint Aircraft Survivability Program in collaboration with Dr. Jaret Riddick of the Vehicle Technology Directorate of APG/Aberdeen. The title of the proposal was "Advanced Composite Materials for Drive Shaft Applications." The proposal was not funded, but another proposal is currently in preparation. The focus of the proposed work is on evaluating the benefits of innovative

material concepts being developed at Penn State for rotorcraft driveshafts. In brief, the work would have evaluated oblique impact under quasi-static torsional loadings on an ARL test rig, using fiber reinforced polymer composite shafts with newly developed nanoreinforcements and flexible matrix materials.

7. Publications and Presentations

Journals:

- Tallman, T. and Wang, K. W., "An Arbitrary Strains Carbon Nanotube Composite Piezoresistivity Model for Finite Element Integration," *Applied Physics Letters*, 102, 011909, 4 p. (2013), doi: 10.1063/1.4774294.
- Zhu, Y., Bakis, C. E., and Adair, J. H., "Effects of Carbon Nanofiller Functionalization and Distribution on Interlaminar Fracture Toughness of Multi-Scale Reinforced Polymer Composites," *Carbon*, 50(3):1316-1331 (2012), doi: 10.1016/j.carbon.2011.11.001
- Tallman, T. N., Gungor, S., Wang, K. W., and Bakis, C. E., "Damage Detection and Conductivity Evolution in Carbon Nanofiber Epoxy via Electrical Impedance Tomography," *Smart Materials and Structures*, 23(4), 045034, 9 p. (2014), doi: 10.1088/0964-1726/23/4/045034.
- Gungor, S., and Bakis, C. E., "Anisotropic Networking of Carbon Black in Glass/Epoxy Composites using Electric Field," *J. Composite Materials*, 10 p. Accepted, available online, Feb. 2014, doi: 10.1177/0021998314521256.

Conferences:

- Zhu, Y., and Bakis, C. E., "CAI Strength of Filament Wound Glass Fiber Composites Toughened with Carbon Nanofillers," *Proc. SAMPE 2012 Conference and Exposition*, Society for the Advancement of Materials and Process Engineering, Covina, CA, 2013, 15 p. (CD-ROM).
- Tallman, T., Semperlotti, F., Wang, K.W., "Enhanced Health Monitoring of Fibrous Composites with Aligned Carbon Nano-Tube Networks and Electrical Impedance Tomography," in *Proceedings SPIE*, Vol. 8348, Health Monitoring of Structural and Biological Systems Conference, 83480G, 2012, 7 p., doi: 10.1117/12.914461.
- Tallman, T, and Wang, K. W., "Analytically Modeling the Piezoresistivity of CNT Composites with Low-Filler Aggregation, in *Proc. SPIE*, Vol. 8692, Sensors and Smart Structures Technologies for Civil, Mechanical, and Aerospace Systems, 869210, 2013, 6 p., doi: 10.1117/12.2008960.
- Gungor, S. and Bakis, C. E., "Electrical Anisotropy of Unidirectional Glass Fiber Reinforced Composites Containing Carbon Black," in *Proc. SAMPE 2013 Conference and Exposition*, Vol. 58, K. M. Storage, T. M. Storage, N. Titchenal and S. W. Beckwith, Eds., Society for the Advancement of Materials and Process Engineering, Covina, CA, 2013, pp. 2091-2099, ISBN 978-1-934551-15-8.
- Tallman, T., Semperlotti, F., and Wang, K. W., "Enhanced Damage Detection in Conductive Polymer-based Composites through Piezoresistive Coupling," *Proc. 28th*

Technical Conference, American Society for Composites, C. E. Bakis, Ed., DEStech Publications, Lancaster, PA, 2013, Paper No. 52, 9 p., (CD ROM).

8. Awards and Honors

C. E. Bakis

- Fellow, American Society for Composites, 9/2010.
- Recording Secretary of the American Society for Composites, 2010 and 2011.
- Vice President, American Society for Composites, 2012 and 2013.
- President, American Society for Composites, 2014 and 2015.

K. W. Wang

- Fellow of the American Association for the Advancement of Science, 12/2010.
- SPIE Smart Structures and Materials Lifetime Achievement Award, 2011.
- Keynote Speaker, International Conference on Vehicle Noise, Vibration and Safety Technology, Chongqing, China, October 2011.
- Plenary Speaker, SPIE Smart Structures/NDE Forum and Conferences, San Diego, CA, March 2012.
- Keynote Speaker, Mechanical Engineering Curricular Models for the Future Plenary, ASME International Mechanical Engineering Education Conference, Clearwater, FL, March 2012.
- Keynote Speaker, the 24th Conference on Mechanical Vibration and Noise, ASME International Design Engineering Technical Conferences, Chicago, IL, August 2012.
- Keynote Speaker, the 36th Conference on Theoretical and Applied Mechanics, Chong Li, Taiwan, November 2012.
- Distinguished Seminar Series Speaker, MAE Department 20th Anniversary Distinguished Seminar Series, Chinese University of Hong Kong, Hong Kong, China, January 2014.
- Plenary Speaker, Smart Materials and Structures Workshop, Harbin Institute of Technology, Harbin, China, January 2014.

9. Graduate Students Involved Directly in ARO Project

- Ye Zhu, Ph.D., Department of Engineering Science and Mechanics, Pennsylvania State University (graduated 12/2011),
- Sila Gungor, Ph.D., Department of Engineering Science and Mechanics, Pennsylvania State University (graduated 12/2013).
- Tyler Tallman, Ph.D. candidate, Department of Mechanical Engineering, University of Michigan (in progress).

10. Cited References

ASTM D5528-01, 2007. Standard test method for mode I interlaminar fracture toughness of unidirectional fiber-reinforced polymer matrix composite. ASTM International, West Conshohocken, PA.

ASTM D 6264, 2007. Standard test method for measuring the damage resistance of a fiber-reinforced polymer-matrix composite to a concentrated quasi-static indentation force. ASTM International, West Conshohocken, PA.

Balberg, I., 2002. A comprehensive picture of the electrical phenomena in carbon black - polymer composites. *Carbon*, 40, 139-143.

Domingues, D., Logakis, E., and Skordos, A. A., 2012. The use of an electric field in the preparation of glass fibre/epoxy composites containing carbon nanotubes. *Carbon*, 50, 2493-2503.

Gao, L., Chou, T. W., Thostenson, E. T., Zhang, Z., and Coulaud, M., 2011. In situ sensing of impact damage in epoxy/glass fiber composites using percolating carbon nanotube networks. *Carbon*, 49, 3371-3391.

Hoa, S. V., and Naghashpour, A., 2013. Method and system for detecting and locating damages in composite structures. International Publication Number: WO 2013/086626 A1.

Hou, T. C., Loh, K. J., and Lynch, J. P., 2007. Spatial conductivity mapping of carbon nanotube composite thin films by electrical impedance tomography for sensing applications. *Nanotechnology*, 18, 315501.

Hou, T. C. and Lynch, J. P., 2009. Electrical Impedance Tomographic Methods for Sensing Strain Fields and Crack Damage in Cementitious Structures. *Journal of Intelligent Material Systems and Structures*, 20, 1363-1379.

Hu, N., Karube, Y., Arai, M., Watanabe, T., Yan, C., Li, Y., Liu, Y., and Fukunaga, H., 2010. Investigation on sensitivity of a polymer/carbon nanotube composite strain sensor. *Carbon*, 48, 680-687.

Hu, N., Masuda, Z., Yamamoto, G., Fukunaga, H., Hashida, T., and Qiu, J., 2008. Effect of fabrication process on electrical properties of polymer/multi-wall carbon nanotube nanocomposites. *Composites: Part A*, 39, 893-903.

JIS K 7086, 1993. Testing methods for interlaminar fracture toughness of carbon fibre reinforced plastics. Japanese Standards Association, Tokyo, Japan, pp. 651-55.

Kang, I., Schulz, M. J., Kim, J. H., Shanov, V., and Shi, D., 2006. A carbon nanotube strain sensor for structural health monitoring. *Smart Materials and Structures*, 15, 737.

Kumar, S., Rath, T., Mahaling, R. N., Reddy, C. S., Das, C. K., Pandey, K. N., Srivastava, R. B., and Yadaw, S. B., 2007. Study on mechanical, morphological and electrical properties of carbon nanofiber/polyetherimide composites. *Materials Science and Engineering B*, 141, 61-70.

Loh, K. J., Hou, T. C., Lynch, J. P., and Kotov, N. A., 2009, Carbon nanotube sensing skins for spatial strain and impact damage identification. *Journal of Nondestructive Evaluation*, 28, 9-25.

Loyola, B. R., Briggs, T. M., Arronche, L., Loh, K. J., La Saponara, V., O'Bryan, G., and Skinner, J. L., 2013. Detection of spatially distributed damage in fiber-reinforced polymer composites. *Structural Health Monitoring*, 12, 225-239.

Mei, Q., Wang, J., Wang, F., Huang, Z., Yang, X., and Wei, T., 2008. Conductive behaviors of carbon nanofibers reinforced epoxy composites. *Journal of Wuhan University of Technology-Material Science Edition*, 23, 139-142.

Naghashpour, A. and Hoa, S. V., 2013. A technique for real-time detection, location and quantification of damage in large polymer composite structures made of electrically non-conductive fibers and carbon nanotube networks. *Nanotechnology*, 24, 455502.

Nofar, M., Hoa, S. V., and Pugh, M. D., 2009. Failure detection and monitoring in polymer matrix composites subjected to static and dynamic loads using carbon nanotube networks. *Composites Science and Technology*, 69, 1599-1606.

Rubin, Z., Sunshine, S. A., Heaney, M. B., Bloom, I., and Balberg, I., 1999. Critical behavior of the electrical transport properties in a tunneling-percolation system. *Physical Review B*, 59, 19, 12196-12199.

Simmons, J. G., 1963. Generalized formula for the electric tunnel effect between similar electrodes separated by a thin insulating film. *Journal of Applied Physics*, 34, 1793.

Tallman, T., Semperlotti, F., and Wang, K. W., 2012. Enhanced health monitoring of fibrous composites with aligned carbon nano-tube networks and electrical impedance tomography. In *Society of Photo-Optical Instrumentation Engineers, Health Monitoring and Structural and Biological Systems Conference*, SPIE, 8348, 83480G (7p.).

Thostenson, E. T., Gangloff, J. J., Li, C., and Byun, J.-H., 2009. Electrical anisotropy in multiscale nanotube/fiber hybrid composites. *Applied Physics Letters*, 95, 073111.

Viets, C., Kaysser, S., and Schulte, K., 2013. Damage mapping of GFRP via electrical resistance measurements using nanocomposite epoxy matrix systems. *Composites: Part B*. http://dx.doi.org/10.1016/j.compositesb.2013.09.049.

Wichmann, M. H. G., Sumfleth, J., Gojny, F. H., Quaresimin, M., Fiedler, B., and Schulte, K., 2006. Glass-fibre-reinforced composites with enhanced mechanical and electrical properties - benefits and limitations of a nanoparticle modified matrix. *Engineering Fracture Mechanics*, 73, 2346-2359.

Zhang, D., Ye, L., Wang, D., Tang, Y., Mustapha, S., and Chen, Y. 2012. Assessment of transverse impact damage in GF/EP laminates of conductive nanoparticles using electrical resistive tomography. *Composites: Part A*, 43, 1587-1598.

Zhu, Y., 2011. Carbon nanofiller modified multifunctional glass fiber/epoxy laminated composites. PhD Dissertation, Penn State University, University Park, PA.

Zhu, Y., and Bakis, C. E., 2012. Damage detection in glass fiber composites using carbon nanofillers and electrical resistance method. *Proc. 2012 SAMPE Intl. Technical Conference*, Society for the Advancement of Materials and Process Engineering, Covina, CA, Paper No. 2431, 14 p. (CD-ROM).